ERA5 REPRODUCES KEY FEATURES OF GLOBAL PRECIPITATION CHANGE IN A WARMING CLIMATE

Omon. A. Obarein[1,2] and Cameron. C. Lee[1,2]

[1] Department of Geography; Kent State University, Kent, Ohio, USA.
[2] ClimRISE Laboratory, Kent State University, Kent, Ohio, USA

Corresponding author: Omon Obarein (oobarein@kent.edu)

325 South Lincoln Street
431 McGilvrey Hall, ClimRISE Lab
Kent, Ohio 44242 USA

Key Points:

- Global precipitation trends from the ERA5 reanalysis aligns with established understandings of precipitation dynamics.
- We find altitudinal stratification of precipitation phase shifts across the Himalayan region.
- Another novel finding is that extreme precipitation trends are not highest during the warmest season, contrary to trends observed in the warmest regions.

Abstract

The largest impact of future climate changes on societies and ecosystems will likely come from precipitation variability and change. In a warming climate, changes in precipitation are governed by complex feedback as the global hydrological cycle intensifies. However, land and water surfaces partition energy and mass differently due to their unique characteristics, making changes over the terrestrial hydrological cycle less straightforward compared to the oceanic phase of the water cycle. Using the ERA5 dataset, this global study examines precipitation trends using eighteen different precipitation parameters across five main components: precipitation total, precipitation frequency, precipitation type, wet and dry spells, and precipitation extreme. Global trends are summarized by land and ocean areas, by climate region, and then zonally averaged to identify broader precipitation patterns and interactions that may not be apparent in local and regional scale studies, especially with a reanalysis dataset. We find that the ERA5 dataset was able to reproduce key features of precipitation change. This study also adds to the growing consensus around other features for which some uncertainty exists. Two surprising findings are that (1) spatial intensification of extreme precipitation around the warmest locations (equatorial region) is not matched by temporal intensification around the warmest time of year (summer months) in the northern hemisphere, and (2) The Himalayas show altitudinal stratification of precipitation phase changes. Finally, with other studies, we find that synoptic weather types may influence the scaling of extreme precipitation with temperature and should be explored in future research.

Plain Language Summary

This study uses the ERA5 dataset to look at how precipitation patterns are changing globally. It looks at 18 different precipitation parameters from five main components, like total precipitation, precipitation frequency, precipitation type, wet and dry spell, and extreme precipitation. The study compares these changes over land and sea, in different climate zones, and globally to understand bigger patterns of change. The main findings are that the ERA5 dataset can capture well-known patterns of precipitation change. Two lesser known findings are that extreme precipitation are increasing in hotter areas near the equator but not during the hottest months in the Northern Hemisphere, and that in the Himalayas, shifts in precipitation type is dependent on altitude. The study also suggests that future research should look at how different weather patterns affect the interaction between extreme precipitation and temperature.

1 Introduction

Precipitation variability and trends are important to climate scientists because of the high-impact nature of precipitation and the potential for that to change in unpredictable and unpleasant ways with climate change (Dai, 2006; Trenberth, 2011 & 2014). Historical changes in precipitation over present and future observations are realized by sub-daily, daily, monthly, seasonal, and interannual variability. The most consistent premise for global precipitation changes over historical observations is that global warming will intensify the global hydrological cycle (Allan et al., 2014; Held & Soden, 2006; Huntington, 2006; IPCC, 2014; Masson-Delmotte et al., 2021; Trenberth, 2014). This theory is due to the strong relationship between water vapor and temperature, based on the Clausius-Clapeyron (C-C) equation, which stipulates a 7% increase in the water holding capacity of the atmosphere for every 1K of warming (Allan et al., 2014; Trenberth, 2011; Vergara-Temprado et al., 2021). Water vapor plays a key role in the regional differences in global precipitation change. Hence, Stephens and Hu (2010) and Trenberth (2011) have noted that total global precipitation changes are predictable to the extent that increases in water vapor are predictable.

Globally-averaged precipitation total is also expected to increase with warming, but at a much-more constrained rate of 2% K^{-1} (Allen & Ingram, 2002; Roderick et al., 2014) because of other dynamic and thermodynamic factors that influence precipitation regardless of the increased moisture-holding capacity of warm air (Westra et al., 2013). However, at the local and regional scale where impacts are felt, this global precipitation sensitivity to warming does not necessarily apply (Roderick et al., 2014). This disparity in precipitation change due to scale is because the intensification of the global hydrological cycle is dominated by the exchanges over the ocean, which is 73% of the Earth's surface. Due to their unique surface characteristics, land and water surfaces respond differently to greenhouse gas forcing and energy and mass partitioning (Byrne & O'Gorman, 2015). Over the ocean, evaporation (E) exceeds precipitation (P), but the surface is still regarded as wet because water is always available for evaporation. Land surfaces, on the other hand, are much more complex. Except in the humid tropics, most land areas are dry (E > P), but precipitation still exceeds evaporation (the bulk of which is generated in the tropics) on average for all land areas as evaporation is constrained by the availability of water (Oke, 2002).

The theory that dry areas will become dryer and wet areas will become wetter, as described by Held and Soden (2006), was based on zonally averaged changes in wetness, which does not hold at the local scale, and especially over land. At most latitudes, P and E are dominated by energy and mass exchanges over the ocean, so their zonal averages (which combined land and ocean surfaces) were determined mainly by oceanic trends (Lim & Roderick, 2009; Oki & Kanae, 2006; Roderick et al., 2014). More recent studies (H. Feng & Zhang, 2015; Greve et al., 2014; Sun et al., 2012) have used empirical studies to dispute this claim, particularly over land areas. So, while regional and local changes are important, precisely what part of the Earth will experience an increase or decrease in precipitation has been the subject of much uncertainty.

Changes in precipitation primarily emphasize precipitation totals, but other components of precipitation are expected to differ in sign and magnitude (Donat et al., 2016; Obarein & Lee, 2022). For example, although global climate models simulate increases in global *mean* precipitation (IPCC, 2014; Masson-Delmotte et al., 2021; Salzmann, 2016), these increases are not as robust as in *extreme* precipitation events (Adler et al., 2017; Emori & Brown, 2005; Sun et al., 2012). The scaling relationship between extreme precipitation and warming suggests a higher sensitivity to increased greenhouse gas forcing than mean precipitation totals (Allen & Ingram, 2002; Chinita et al., 2021; Lehmann et al., 2018). Relative to mean global precipitation totals, extreme daily precipitation consistently shows significant increases in historical observations and has become a near-universal feature of climate model simulations of the planet's response to increasing atmospheric greenhouse concentrations (Bao et al., 2017; Donat et al., 2016). It is expected that extreme precipitation will intensify spatially (over the humid tropics) (Utsumi et al., 2011; Visser et al., 2020), but whether it intensifies at the same rate temporally (over the summer season) remains unclear. Moreover, it is not known whether zonally averaged changes will be dominated by the ocean at the same rate as with precipitation totals.

Furthermore, changes to precipitation frequency, precipitation type, and wet and dry spells are expected to accompany a warming climate and may likely carry a different signal of change than precipitation totals. With respect to precipitation type, decreases in the proportion of precipitation falling as snow have been reported in almost every part of the mid-and high

latitudes (Matiu et al., 2021; Screen & Simmonds, 2012; Shi & Liu, 2021). Over the Arctic, there is growing consensus that precipitation is increasing, consistent with an amplified warming climate (Bintanja & Selten, 2014; McCrystall et al., 2021; Serreze & Barry, 2011), but most of these studies involve precipitation totals. Little is known about the changes in the frequency of snow and rain days (since frequency and totals can differ in magnitude and sign). If precipitation frequency decreases as total increases, extreme precipitation may increase in the region, a trend more associated with warmer climates.

This study evaluates how well the ERA5 reanalysis precipitation dataset reproduces some well-known features of global precipitation change described above. The aim here is to add to the growing consensus around specific signals of change and to draw attention to other features of global precipitation change that are still unclear or have not received enough focus, some of which have been highlighted above. While previous analyses of global precipitation focus on a mean pattern of precipitation totals, this study goes further to fully characterize precipitation by examining eighteen precipitation parameters.

Finally, for all the benefits of local or regional studies, a comprehensive global overview of precipitation change can help identify patterns and anomalies that may not be apparent at the local and regional scales. Global trends are zonally averaged, subdivided by land and ocean areas, and summarized by climate region to identify links with broader climate dynamics and teleconnections. This study also serves as a valuable evaluation of the ERA5 reanalysis precipitation dataset at the global level. Regional and local evaluations are more common but appear skewed towards areas with a dense network of observation stations, mainly in Europe and Asia.

2 Materials and Methods

2.1 ERA5 Reanalysis precipitation dataset

This study uses global hourly precipitation total and precipitation type data (1979 to 2022) from the ERA5 reanalysis, the most recent in the line of European Center for Medium-Range Weather Forecasts (ECMWF) reanalysis products (Hersbach et al., 2020). The dataset has a spatial resolution of 0.25° x 0.25° and covers the globe from 1940 to the present. ERA5 combines vast

historical observations from many sources (station data, satellite data, etc.) into global estimates using advanced modeling and data assimilation systems. The ERA5 is a considerable improvement over the ERA-Interim and other previous ECMWF reanalysis because it assimilates observations from more recent sophisticated weather satellite instruments (Hoffmann et al., 2019; Olauson, 2018; Urraca et al., 2018)

Over the ocean and in many tropical and polar regions, in-situ observations are sparse or unavailable to meet the needs of global studies (Kidd et al., 2010; Thackeray et al., 2022). Most satellite products also tend to have coarse resolution, making them inadequate to capture precipitation variation over short distances, such as in regions of complex topography. Reanalysis datasets can mitigate these problems by providing homogenous and consistent long-term data on regularly spaced temporal and spatial intervals. Most evaluations of ERA5 reanalysis precipitation dataset show high performance in outperforming other reanalysis and satellite-based products (Centella-Artola et al., 2020; Gleixner et al., 2020; Jiao et al., 2021; Malayeri et al., 2021; Nogueira, 2020; Obarein & Lee, 2022; Randriatsara et al., 2022; Wang & Zhao, 2022, and others). This high performance has led to the growing use of the ERA5 dataset in precipitation trend analysis (e.g., Boisvert et al., 2023; Box et al., 2019; Chinita et al., 2021; Yu & Zhong, 2021).

2.2 Precipitation Components

This study utilizes five precipitation components, subdivided into eighteen parameters (Table 1), to exhaustively examine global precipitation change. To derive annual precipitation totals, hourly precipitation is summed for each year of the study area. Summer, winter, fall, and spring totals were derived from seasonal accumulations of hourly precipitation.

Following the recommendation of the WMO (2017), a wet day is defined as one with any daily precipitation totals ≥ 1 mm. Annual wet and dry days are yearly sums of all days ≥ 1 mm and ≤ 1mm, respectively. The annual count of summer and winter wet and dry days are the subset of annual wet and dry days in each year's summer and winter seasons.

171 ***Table 1**: Precipitation components and parameters used in the study.*

S/N	Precipitation components	Parameters (Annual time steps)	Unit 172
1	Total Precipitation	Precipitation total	mm
2		Summer precipitation total	mm
3		Winter precipitation total	mm
4		Spring precipitation total	mm
5		Fall precipitation total	mm
6	Precipitation Type	Rain days	days
7		Snow days	days
8	Precipitation Frequency	Wet days	days
9		Dry days	days
10		Summer wet days	days
11		Summer dry days	days
12		Winter wet days	days
13		Winter dry days	days
14	Wet Spell	Wet Spell	events
15	Extreme Precipitation	Maxima precipitation	mm
16		95^{th} percentile precipitation	mm
17		Count of ≥ 95^{th} percentile precipitation	days
18		Mean of ≥ 95^{th} percentile precipitation	mm

173 "Precipitation Type" was derived from the ERA5 hourly precipitation type dataset, from which
174 only rain and snow are considered in this study. The modal precipitation type that is rain or
175 snow—over any twenty-four-hour period—was regarded as that day's precipitation type, and
176 this was used to generate a categorical time series of precipitation types, from which annual
177 counts of rain and snow days are created. These annual counts of precipitation types only
178 considered days where precipitation was≥ 1mm. ERA5 snowfall is measured in meters of water
179 equivalent. We define a wet spell as an event with two or more wet days following Huang et al.
180 (2017), Chaudhary et al. (2017), Vaittinada Ayar and Mailhot (2021), and others.

181 Extreme precipitation is assessed using four parameters. Annual maxima precipitation is the
182 yearly time series of the highest daily precipitation in a year. An annual wet day 95^{th} percentile
183 index, where percentiles are only expressed relative to wet days (e.g., Kendon et al., 2014; Turco
184 & Llasat, 2011), was used to characterize extreme precipitation. Further, a single wet day 95^{th}
185 percentile precipitation value for the study period was generated and compared to each yearly

distribution to derive a count of all days where the daily precipitation exceeds this 95th percentile value. The fourth extreme precipitation parameter is the mean of all the daily precipitation each year that exceeds the 95th percentile value. Single annual values can have high variability, so the means are calculated as a more robust measure of extreme precipitation. The global climatology of all eighteen precipitation parameters is shown in Figure A1.

2.3 Trend Analysis

Precipitation does not follow a normal distribution, and daily precipitation tends to be negatively skewed due to many non-precipitation days (about 50% and as much as 95% in dry areas) (Burt et al., 2009; Contractor et al., 2021; Pendergrass & Knutti, 2018). As precipitation accumulates over longer timescales, these statistical tendencies tend to diminish due to more non-zero accumulations, but they are still far from a normal distribution. The considerable spatial variability and range of precipitation on a global scale also present challenges for trend analysis. A small change in a dry area may be more significant—especially if variability is low—than a large change in a wet area if variability is high. The large trend value in the latter tends to overshadow the small magnitudes of change in the former, making them incomparable across grid points. To solve this problem, all precipitation parameters are first rendered to a common annual time scale so that the number of observations is equal in each case and comparability across parameters is boosted. Secondly, all the precipitation parameters are standardized using the standardized anomalies or z-scores. Trends performed using the standardized anomalies have units of standard deviation and are comparable across space regardless of the amount and distribution of precipitation.

The magnitude and sign of precipitation change for each parameter were calculated using the Theil-Sen slope estimator—the most widely used nonparametric method for estimating the magnitude of a linear trend (Chervenkov & Slavov, 2019; El-Shaarawi & Piegorsch, 2002). This method is more robust, efficient, and unbiased by outliers than the ordinary least squares method (Dang et al., 2008; Ohlson & Kim, 2015). The Theil-Sen slope method fits a line to a set of points that chooses the median slope among all lines connecting all possible pairs of two-dimensional sample points.

The statistical significance of each trend value from the Theil-Sen slope estimator was calculated using the nonparametric Modified Mann-Kendall (MK) trend test. This test is distribution-independent but is equally robust and less sensitive to outliers and missing values comparatively to other trend tests (Ali et al., 2019; Liu et al., 2016; Şen, 2017). It is routinely used in hydro-climatological datasets and is recommended by the WMO (Liu et al., 2015, 2016). More importantly, the modified MK test builds upon the original Mann-Kendall by accounting for serial autocorrelations that climatic datasets may exhibit (Hamed & Ramachandra Rao, 1998). Unlike the original Mann-Kendall trend test, the modified MK test only calculates statistical significance using the standard normal test statistic Z, and p-values for each grid point. The Z statistic is denoted as.

$$z = \begin{cases} \dfrac{S-1}{\sqrt{\dfrac{n(n-1)(2n+5)}{18}}} & \text{if } S > 0 \\ 0 \text{ if } S = 0 \\ \dfrac{S+1}{\sqrt{\dfrac{n(n-1)(2n+5)}{18}}} & \text{if } S < 0 \end{cases} \quad (1)$$

Where $|Z| \geq Z_{1-\alpha/2}$, the null hypothesis is rejected at the 95% confidence level, and a significant trend exists in the dataset. Theil-Sen slope estimator and the Mann-Kendall trend test are calculated for all precipitation parameters in Table 1, separately for all grid points, using MATLAB.

Conducting multiple hypothesis tests (like above) often leads to misinterpretation of statistical significance, as it increases the rate at which a true null hypothesis is erroneously rejected [called the False Discovery Rate (FDR)]. The procedure that Wilks (2016) described to control for the FDR uses the "field significance" approach that requires a higher standard (smaller p-values) to reject the null hypothesis at each individual grid point in order to maintain the stated α-level considering the multiple tests being conducted. Herein, Wilks' FDR is calculated in MATLAB for every trend analysis.

Trends are averaged by latitude and subdivided into land and ocean grid points. Also, trends are summarized based on the six Köppen-Geiger global climate classification system to identify any important regional differences in results.

When dealing with global gridded climatic datasets, especially on square grids, the physical area represented by each grid varies. Near the equator, a square degree of latitude and longitude represents a larger area than it does at the poles. When aggregating data over grids, this area disparity gives undue weight to high-latitude regions. To solve this issue, we use a resampling technique that selects representative equal-sized/spaced grid points at coarser resolutions. This resampling is done in MATLAB.

3 Results

This study's findings are discussed under four subsections, each underscoring salient aspects of global precipitation change. Notably, these results align with established understandings of precipitation dynamics, yet their replication using the ERA5 reanalysis dataset adds a layer of significance. Within these sections, the study delves into more intricate and previously unexplored phenomena. These include the nuanced altitudinal stratification of precipitation phase shifts across the Himalayan region, as well as the temporal variation in extreme precipitation events. Such insights offer a novel contribution to the existing body of literature in this field.

3.1 *Near total increase in extreme precipitation, but highest in the deep tropics.*

Among all precipitation parameters, extreme precipitation (annual maxima, 95^{th} percentile precipitation, count of $\geq 95^{th}$ percentile precipitation, and mean of $\geq 95^{th}$ percentile precipitation) distinctly shows near-total increasing trends, with only small pockets of decreasing trend (Figure 1o to 1r).

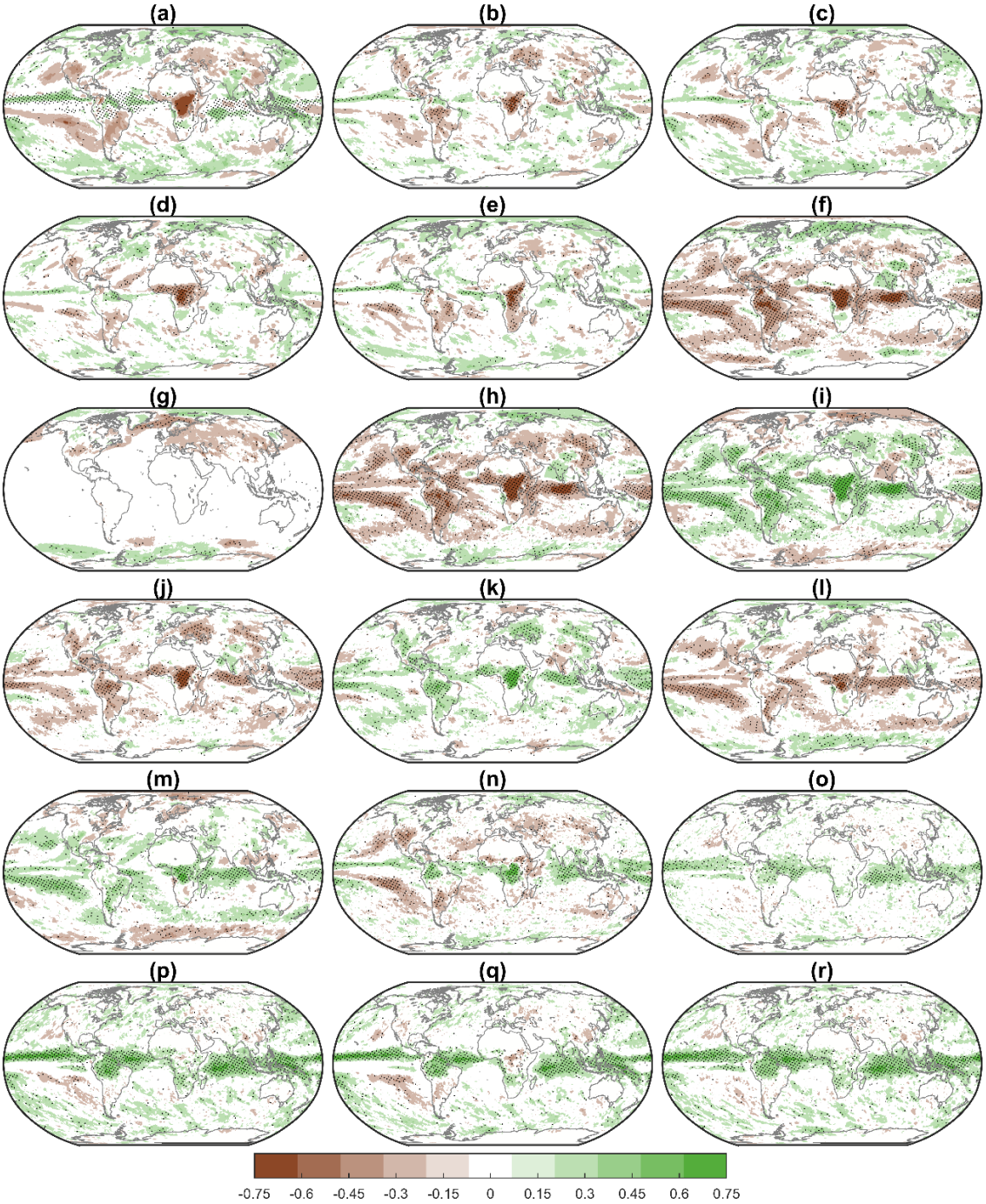

***Figure 1**: Global trends (1979 - 2022) in (a) Annual precipitation totals; (b) Annual JJA precipitation totals; (c) Annual DJF precipitation totals; (d) Annual MAM precipitation totals; (e) Annual SON precipitation totals; (f) Annual rain days; (g) Annual Snow days; (h) Annual wet days; (i) Annual dry days; (j) Annual summer wet days; (k) Annual summer dry days; (l) Annual winter wet days; (m) Annual winter dry days; (n) Annual wet spell; (o) Annual Maxima precipitation; (p) Annual 95th percentile precipitation; (q) Annual count of ≥ 95th percentile precipitation; and (r) Annual mean precipitation ≥ 95th percentile precipitation. Black stippling indicates statistically significant grid points. All trends are decadal and in standard deviation (z-scores) units.*

The narrow band of strong and significant trends near the equator is consistent with sharp zonally averaged increases around the equatorial region (Figure 2).

The equatorial region is experiencing the largest increases in extreme precipitation over the last four decades. Near the equator, the positive trend in the 95th percentile precipitation and the mean of all precipitation ≥ 95th percentile precipitation are nearly four times the trend in the subtropics (Figures 2a and 2d). This four-fold difference amounts to a 0.45 σ/decade increase from the mean 95th percentile precipitation and the mean number of precipitation days ≥ 95th percentile precipitation.

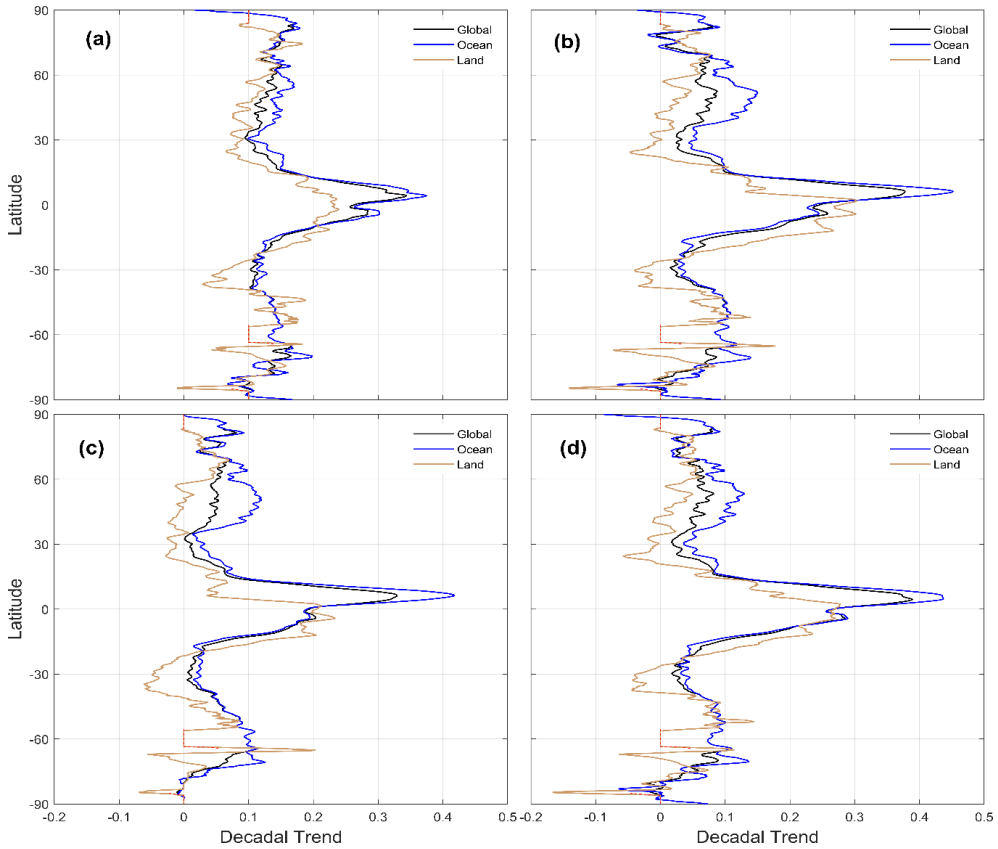

Figure 2: *Global trends averaged by latitude, and sub-divided into global, ocean, land grid points, for (a) annual maxima precipitation; (b) annual 95th percentile precipitation; (c) annual count of precipitation event ≥ 95th percentile precipitation; and (d) annual mean precipitation ≥ 95th percentile precipitation. The red line represents the absence of land grid-points. Decadal trends are in standard deviation (z-score) units.*

The decreases in extreme precipitation in the subtropics—centered around 30^0 North and South—set up a sharp latitudinal gradient with the equatorial region that is observable when

trends are summarized by climate region. Table 2 shows the 25th percentile trend value in annual maximum precipitation and annual mean precipitation ≥ 95th percentile precipitation. This trend value is positive only in the tropics, indicating that the top 75th percentile of extreme precipitation are all positive for the region. Other climate regions do not show this positive skewness in extreme precipitation trends

***Table 2**: 25th percentile extreme precipitation trend value in each climate region*

Climate Region	Ann max	Mean 95th
Tropical	0.0207	0.0207
Dry	-0.0466	-0.0466
Mesothermal	-0.046	-0.046
Microthermal	-0.0486	-0.0486
Polar	-0.029	-0.029
Highland	-0.0807	-0.0807

Within this broad zonal gradient, variation by land and ocean surfaces is apparent everywhere: Figure 1 and 2 show lower magnitudes of change in extreme precipitation over zonally-averaged land areas compared to ocean surfaces across all four extreme precipitation parameters. The prominent increasing trends over the deep tropics are dominated by trends over the ocean, which can be twice as much as those over land. This land-ocean contrast is seen across all extreme precipitation parameters, except annual maxima precipitation in the Northern Hemisphere mid-latitudes. And while oceanic trends in the subtropics are small (but still positive), the land trends show a decreasing trend. Zonally-averaged trends in all eighteen components are shown in Supplementary Figure A3.

The increase in precipitation extremes with global warming is currently the biggest signal of precipitation change, consistent with theory (Allen & Ingram, 2002; Trenberth et al., 2003), observational studies (Ribes et al., 2019; Westra et al., 2013), and climate model simulations (O'Gorman & Schneider, 2009; Pendergrass & Hartmann, 2014). Of all precipitation components, extreme precipitation scales the most with temperature, almost approaching the (C-C) scaling rate of atmospheric moisture with temperature (7% per $^{0}C^{-1}$) (Chinita et al., 2021; Lehmann et

al., 2018), the highest possible rate of increase in precipitation with global warming in theory, all other factors being equal. This scaling relationship is confirmed in Figure 3, where the timeseries of globally-averaged standard deviations of annual 95th percentile (extreme) precipitation increased fastest with temperature trends relative to other precipitation components. Studies have however shown that hourly precipitation extremes can exceed this maximum rate (Prein et al., 2017; Visser et al., 2020; Westra et al., 2014).

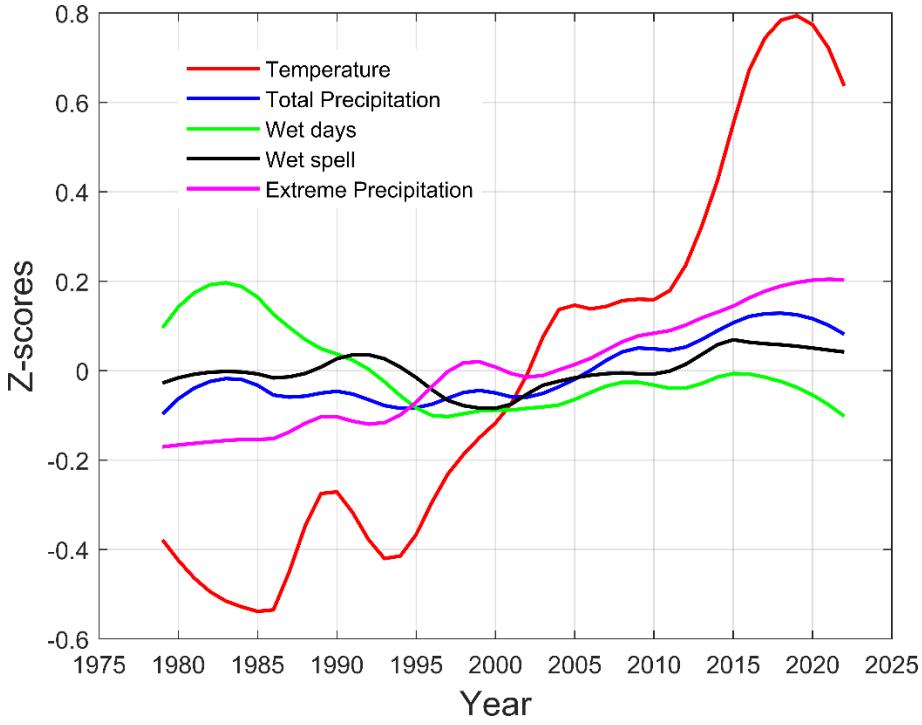

Figure 3: *Globally-averaged standard deviations of mean annual temperature, annual total precipitation, annual wet days, annual wet spell, and extreme (95th percentile) precipitation (1979 – 2022).*

Scaling rate strongly depends on heat and moisture availability, two quantities abundantly available in the equatorial oceans, which explains statistically significant increases in the region. Over tropical land areas where temperatures are equally high, the limitation of moisture and the complication of a heterogeneous surface constrains increases in extreme precipitation below those over the ocean, where water is always available.

Like the ocean-land contrast, the latitudinal variation in extreme precipitation changes also aligns with findings in previous studies (Fischer et al., 2014; Kharin et al., 2013) and is very well explained by latitudinal variations in the scaling of extreme precipitation with temperature. For

instance, Pfahl et al. (2017) showed that the spatial pattern of scaling is highly correlated with the spatial distribution of changes in precipitation extremes, including over the subtropics where decreasing trends in precipitation were simulated.

Fewer studies have explicitly explored *seasonal* variation in scaling rates and potential implications for precipitation extremes. Schroeer and Kirchengast (2018) found that extreme precipitation had a lower scaling rate during the summer than in the spring and fall seasons. Their result seemed counterintuitive because precipitation extremes intensify with warmth over the deep tropics which would intuitively lead one to think that scaling would be greatest in the summer months, the warmest season in the Northern Hemisphere (Figure A2). To test this hypothesis, trends in the seasonal count of days exceeding the 95th percentile of precipitation are calculated over all four seasons and averaged across all Northern Hemisphere grids (Figure 4). Consistent with Schroeer and Kirchengast's (2018) result, we found that while extreme precipitation is increasing across all seasons, the summer months surprisingly showed the joint lowest rate of increase. Schroeer and Kirchengast (2018) explained that certain dynamic factors, such as moisture advection and other atmospheric circulation patterns, modulate the scaling of extreme precipitation with temperature, especially in the warmest months. Other studies have noted that departures from the C-C scaling often result from changes in circulation patterns and synoptic weather systems (Allan et al., 2014; Martinkova & Kysely, 2020), but these have not been fully explored. Therefore, further research on how the temperature sensitivities look in different weather types is needed to provide valuable insight into the dynamic controls of the temperature-precipitation scaling on a regional to local-scale.

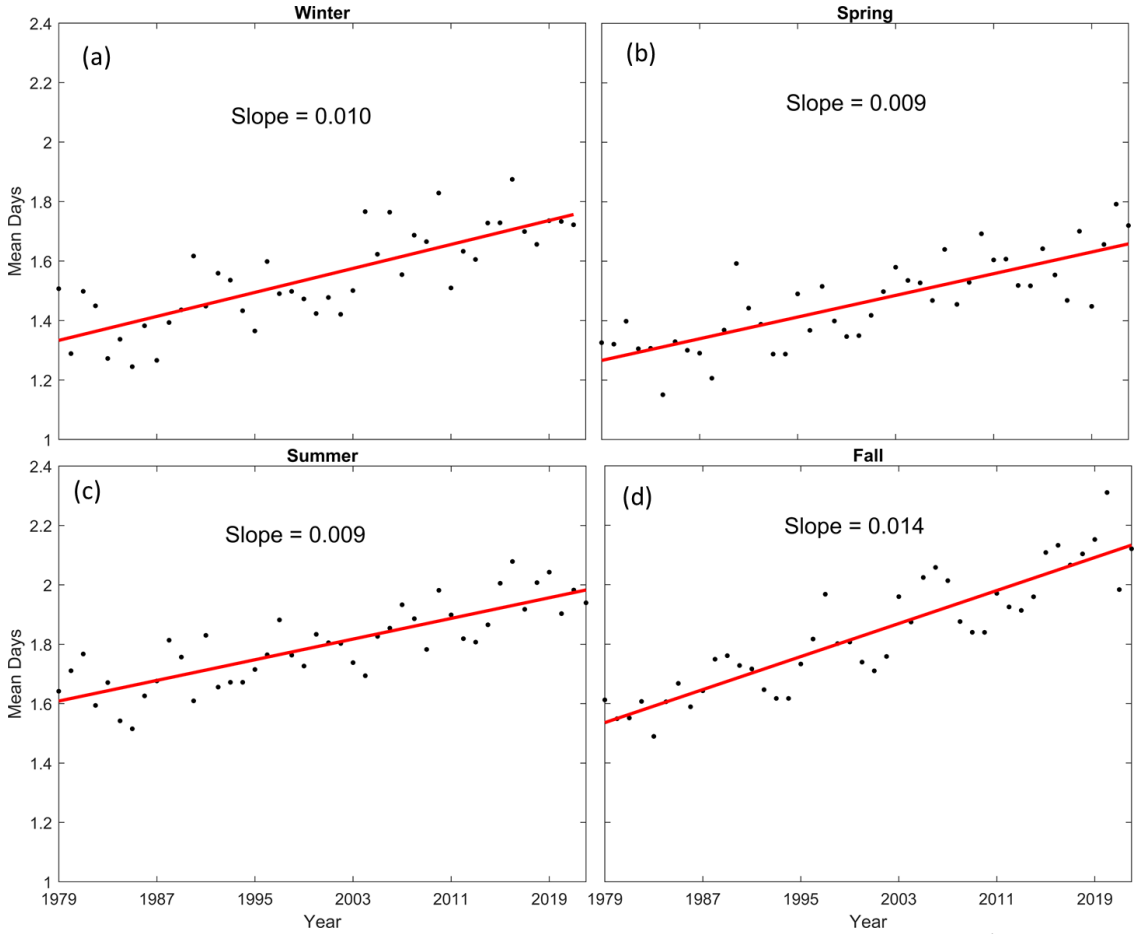

***Figure 4**: Mean annual number of days with precipitation ≥ the seasonal 95th Percentile precipitation in (a) Winter (DJF), (b) Spring (MAM), (c) Summer (JJA), and (d) Fall (SON) for the Northern Hemisphere*

3.2 Precipitation is increasing in the Arctic region

To reveal changes in precipitation over the Arctic region, Figure 5 visualizes trends in selected precipitation parameters with a polar projection centered around the Arctic. The results show increasing trends in annual totals, wet days, snow days, and wet spells. The decreasing trend in dry days is also consistent with a general uptick in precipitation amount and frequency in the region.

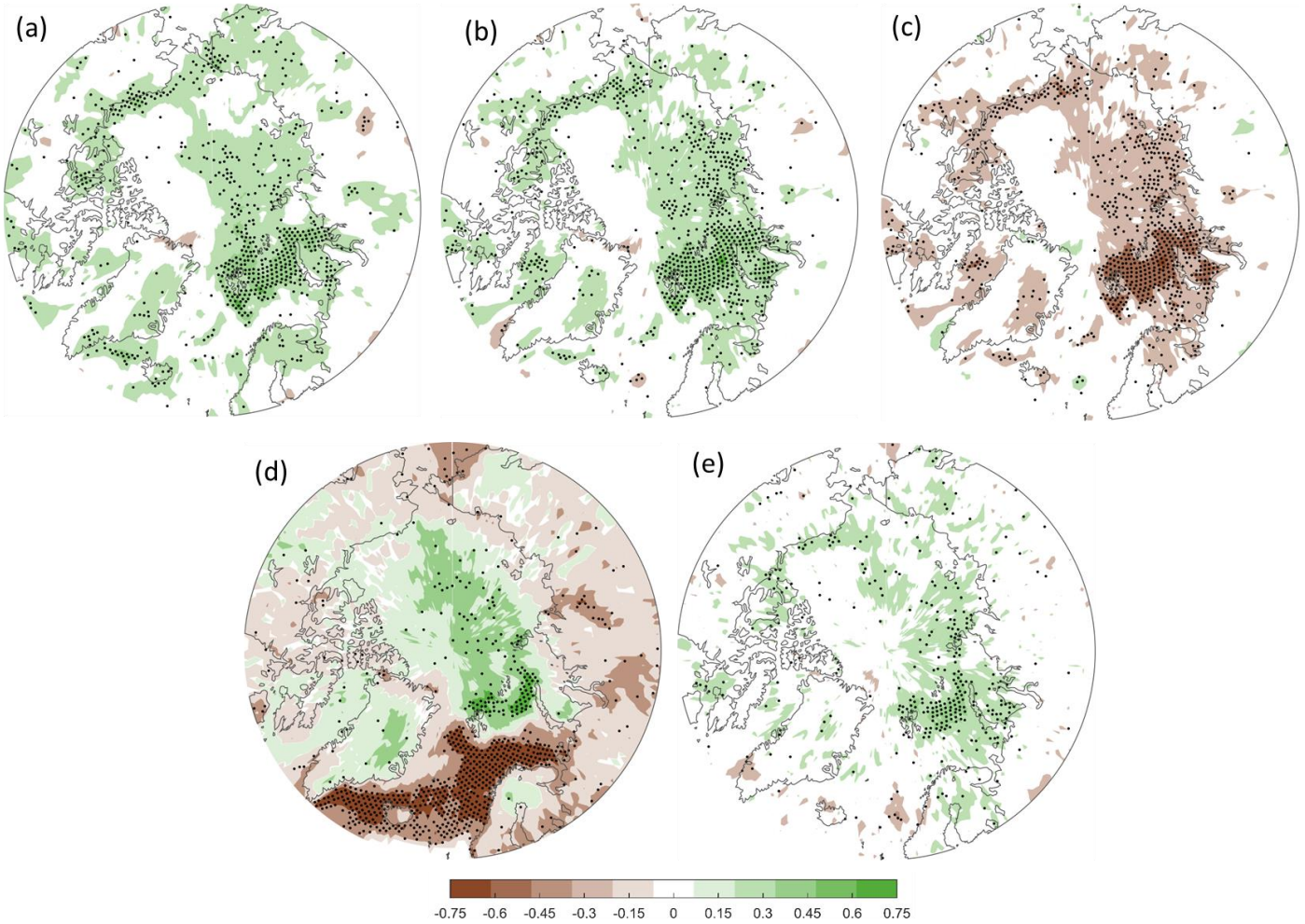

Figure 5: *Azimuthal projection centered around the Arctic showing trends in (a) annual precipitation total; (b) annual count of wet days; (c) annual count of dry days; (d) annual snow days; and (e) annual count of wet spell. Black stippling indicates statistically significant grid points. All trends are decadal and in standard deviation (z-scores) units.*

These trends are most prominent over the central and Eastern Arctic region and over the Barents Sea. When trends in these parameters are subdivided by regions, results over the Arctic are consistent with the positive trends found in polar climates (Figure 6). It is shown that, except for annual snow days, the top 75th percentile of trends in polar climates—dominated by trends over the Arctic since Antarctica has little to no trends—are positive. Increasing trends in annual snow days are limited to the Central Arctic and Greenland because of the massive, statistically significant decreasing trend over the Norwegian, Barents, and Greenland Seas—the bodies of water separating Greenland from Europe and Asia. Supplementary Figure A4 shows trends subdivide by regions for all eighteen precipitation parameters.

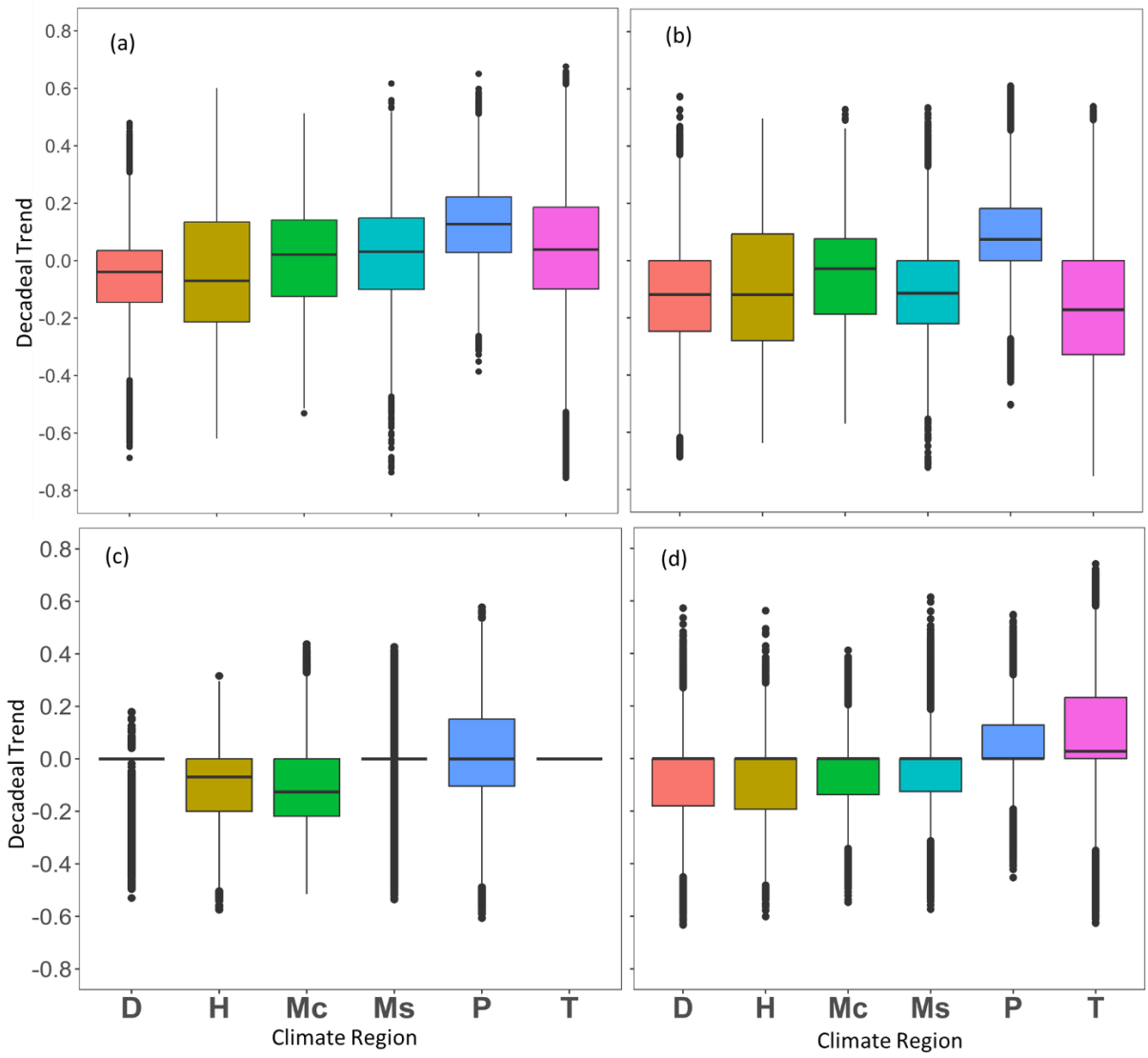

Figure 6: *Global trends by climate region in (a) annual precipitation, (b) annual count of wet days, (c) annual snow days, and (d) annual count of wet spell. All trends are decadal and in standard deviation (z-scores) units. Climate Region: T = Tropical; D = Dry Climate; Mc = Microthermal Climate; Mesothermal Climate; P = Polar Climate; H = Highland Climate)*

Our results are consistent with the general scientific consensus that Arctic amplification is driving the observed increasing trend in precipitation over the Arctic (Boisvert et al., 2023; Box et al., 2019; Yu & Zhong, 2021). Climate modeling studies also predict that these increases will persist at least until the end of the 21st century (Parker et al., 2022; Webster et al., 2021). It well known that precipitation increases with warmer temperatures but at different rates, depending on regional and local temperature and moisture availability, as well as the modulating dynamic and thermodynamic controls (Gu et al., 2023; Tan et al., 2023).

The Arctic is warming nearly four times the global average (Jacobs et al., 2021; Rantanen et al., 2022). Two main arguments have been proposed to explain the physical processes driving this warming-induced precipitation over the Arctic. The first is related to ice-albedo/insulating feedback, where higher temperatures lead to decreases in sea ice concentration and thickness, increasing evaporation from an exposed ocean surface, ultimately leading to precipitation increases from greater atmospheric moisture. This mechanism has been shown in observational evidence (Kopec et al., 2016) and modeling studies (Cai et al., 2021; Landrum & Holland, 2020). The second explanation for warming-induced precipitation increases over the Arctic is enhanced moisture transport from lower latitudes, primarily due to a waiver jet stream that permits moist air intrusion, leading to sea-ice retreat (Francis & Vavrus, 2015; Woods & Caballero, 2016). Bintanja (2018) estimates that these two mechanisms will account for 50 – 60% of the increase in Arctic precipitation over the 21st century.

The Arctic is one of the most challenging places to collect in-situ observations because of its remote location, harsh weather conditions, and extreme cold, leaving reanalysis datasets as the only viable data source for observational precipitation studies. Remarkably, there has been agreement between observational studies and model simulations of precipitation change in the Arctic.

3.3 More precipitation falls as rain than as snow (in mid-and high-latitudes) except in the Arctic

Most of the mid- and high-latitude regions of the Northern Hemisphere, particularly over the vast Eurasian land mass, are experiencing decreasing trends in the annual number of snow days, some of which are statistically significant (Figure 7a). Consistent with the density of statistically significant grids, the strongest decreasing trends are found in the Norwegian and Greenland Seas—the intervening body of water between Greenland and Europe, just outside the Arctic Circle. Over the major mountain ranges on Earth (the Himalayas, the Alps, the Andes), decreasing snow days prevail. There is a broad region of statistically significant decreasing trends in snow days encompassing the Rockies and Great Plains of the US.

Over the Arctic, the increasing trends in snow days are consistent with the general increasing trend in precipitation in the region discussed in the preceding section. Other noteworthy locations of increasing trend are western and southwestern Canada and the Southern Ocean.

To further analyze these snow day trends, Figure 7b displays the locations where the median precipitation type over the first half of the study (1979 - 2000) changed to another median precipitation type during the second half of the study (2001 – 2022). The result indicates that most locations with statistically significant decreasing trends have shifted from median snow days to median rain days. These locations represent about 3% of mid- and high-latitude surface area. By contrast, locations with a median shift from rain to snow account for only 1% of mid- and high-latitude surface. Surprisingly, this shift to a snowfall regime co-occurs with decreasing snow days over the Gobi Desert—a cold desert in Mongolia and China (Figure 7b). A shift from rainfall to snowfall without a corresponding increase in snow days is possible if the intensity or amount of snowfall increases in fewer days of precipitation. It should be noted that these shifts are based on the frequency of precipitation types and not totals.

Another surprising result is that over the Himalayas, the shift from snowfall to a rainfall regime occurs over lower elevations, but the peaks show no change. This scenario suggests a microclimate effect where the highest elevations still receive consistent snowfall while transitional zones see more rainfall as mean temperatures rise.

Decreases in the proportion of precipitation falling as snow have been reported in almost every part of the mid-and high latitudes: the Arctic (Screen & Simmonds, 2012), western and contiguous US (Feng & Hu, 2007; Huntington et al., 2004; Knowles et al., 2006; Shi & Liu, 2021); Canada (Han et al., 2018); Tibetan Plateau (Wang et al., 2016); Europe (Blöschl et al., 2019; Matiu et al., 2021; Rixen & Rolando, 2013); and the whole world (Shi & Liu, 2021). Although not examined in this study, a seasonality in precipitation type shift has been reported by Wrzesien et al. (2022). Even with warming, winter temperatures are still cold enough the high-latitudes that precipitation will fall mainly as snow, so changes in precipitation type are expected to be more pronounced in fall and spring, explaining why we show increases in both snow days and rain days. It is still likely that the proportion of precipitation falling as snow has decreased annually.

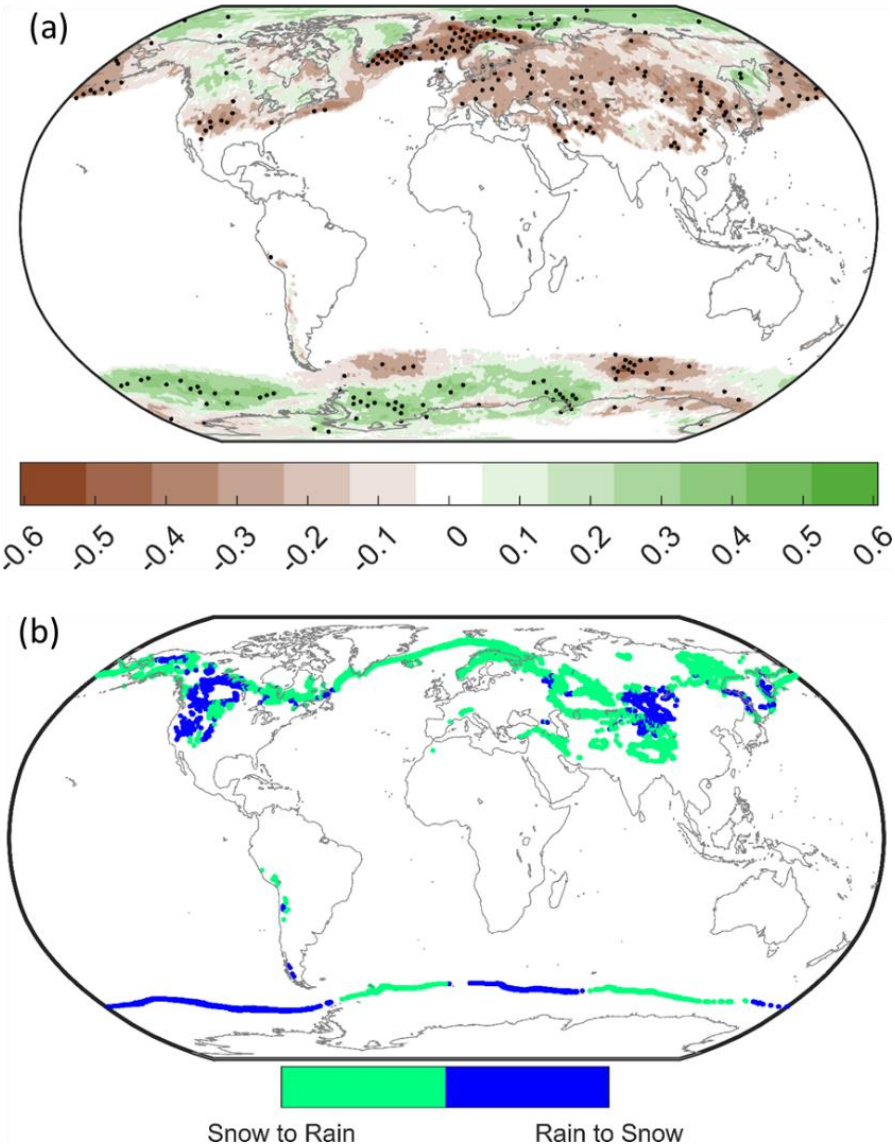

Figure 7: (a) *Annual trends in snowfall days (1979 - 2022) (Black stippling indicates statistically significant grid points). All trends are decadal and in standard deviation (z-scores) units.* ***(b)*** *Locations where median precipitation type shifted from snow to rain and from rain to snow between the first half (1979 -2000) and the second half (2000 – 2022) of the study period.*

The result over the Tibetan Plateau is supported by Jouberton et al. (2022), who recently reported warming-induced shifts to a rainfall regime over lower elevations in the southeastern Tibetan Plateau that gets significant monsoon precipitation. Because snow and ice—especially in mountainous regions—are sensitive indicators of a warming climate (Hynčica & Huth, 2019) and vital sources of freshwater, a shift to a predominantly rainfall regime over the Himalayas has crucial implications for energy budgets, water resources and management, ecology, and many

other important entities. It is not surprising that the Himalayas have been referred to as the "third pole" because it holds the largest snow and ice cover outside the polar regions and mimics Arctic and Antarctic environmental and climatic characteristics and significance (Banerjee et al., 2021; Pant et al., 2018).

3.4 Tropical Land and ocean contrast in the sign and magnitude of change in precipitation total and frequency

The left pane of Figure 8 shows the spatial distribution of trends in annual precipitation totals, annual summer precipitation totals, and annual wet days. The corresponding latitudinal variation of the land and ocean components of these trends are shown on the right pane. The results show that most land areas, especially in the tropics, are experiencing a strong statistically significant decreasing trend. Hence, while precipitation changes over the ocean dominate globe-wide changes in extreme precipitation, this tendency is more pronounced in precipitation totals and frequency. The biggest difference is in annual wet days, where, in addition to the difference in sign of change, the magnitude of the decreasing trend over land is nearly two times the increasing trend over the ocean. Also, the decreasing trend over land spans a wider latitudinal range for annual wet days. Over the maritime continent, the increasing trends in precipitation totals and frequency disappear in wet day trends, explaining the intensification of extreme precipitation in that region.

A clear disparity in the response of the terrestrial and oceanic water cycle to global warming has been reported by many scholars (Berg et al., 2016; Fasullo, 2010). However, there has been much uncertainty about the dynamical processes that explain this disparity and their representation in climate models (Byrne & O'Gorman, 2015). While thermodynamic processes have been accounted for in future climate models, mechanisms of dynamical changes are not easily explained or well represented (Neelin et al., 2022). These dynamical changes (such as those associated with changes in convergence, atmospheric circulation and the movement of air masses, eddies and storms, advection, winds, etc.) that modulate the complex land/vegetation-atmosphere feedbacks which amplify aridity over land have not been well accounted for (Berg et al., 2016).

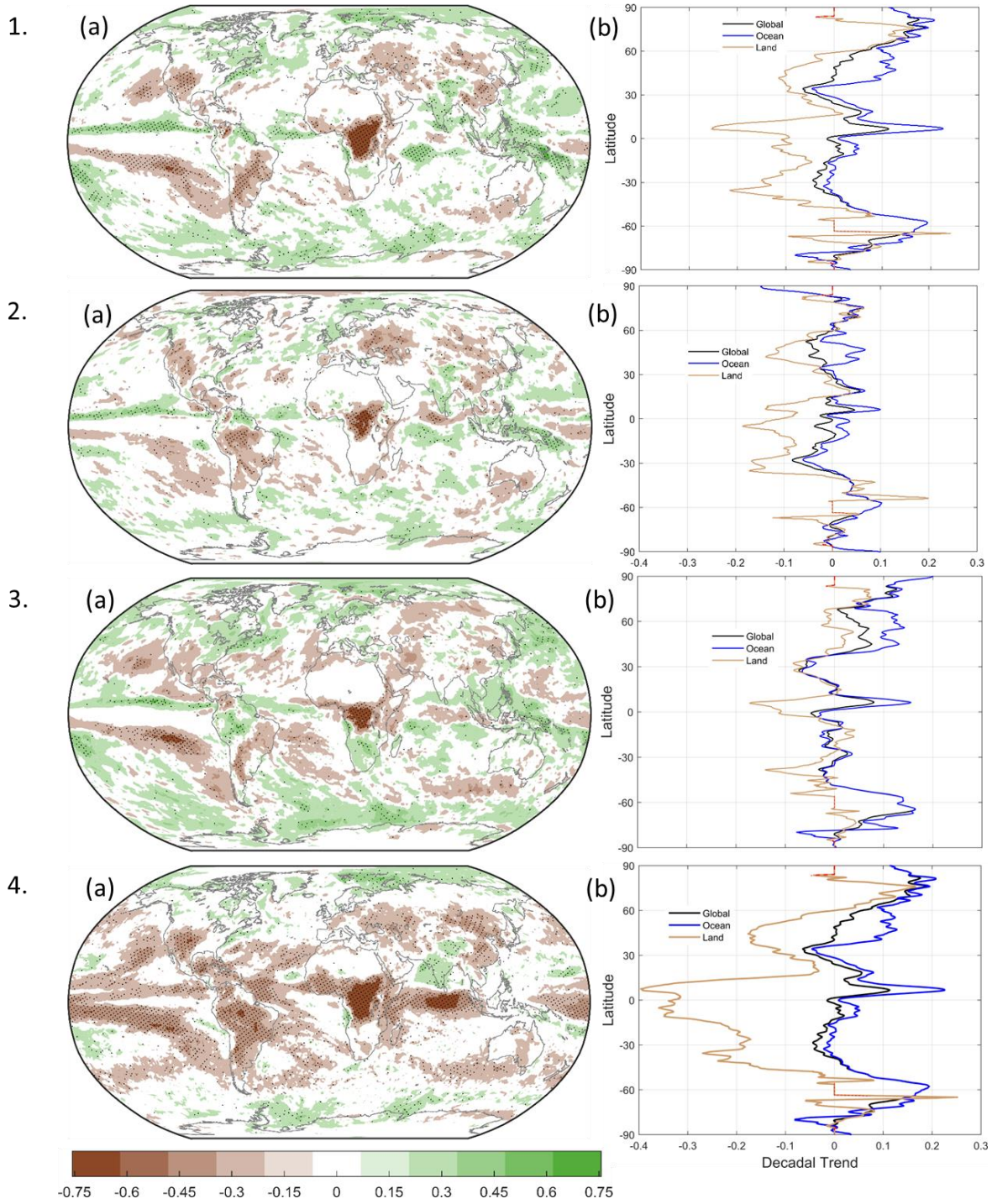

Figure 8: *Global trends (Left) averaged by latitude and subdivided into global, ocean, and land grid points (right) for (1) annual total precipitation, (2) annual total JJA precipitation, (3) annual total DJF precipitation, and (4) annual wet days. Black stippling indicates statistically significant grid points. All trends are decadal and in standard deviation (z-scores) units.*

On a global scale, the most popular mechanism put forward to explain the spatial variation of precipitation change is the "wet-get-wetter, dry-get-drier" mechanism—called the direct moisture effect—popularized by, Held and Soden (2006), Chou et al. (2009), and Trenberth (2011). The direct moisture effect – based on the simple scaling of water vapor with temperature – applies more to extreme precipitation than to totals and frequency, and is robust over the ocean (Feng & Zhang, 2015; Greve et al., 2014; Sun et al., 2012). The greater robustness of this mechanism over the ocean compared to land is a consequence of the greater physical basis of the simple scaling of water vapor with temperature in the former than in the latter (Byrne & O'Gorman, 2015; Held & Soden, 2006). Overland, dynamical systems, which are more regional and dependent on land complexities and circulation and advection, are not represented in the thermodynamic scaling of the atmospheric moisture convergence, which underlies the direct moisture effect (Byrne & O'Gorman, 2015).

This decreasing trend in precipitation totals and frequency discussed above is primarily driven by drying trends in the Congo Basin of Central Africa. Figure 8 (and also Figure 1f, 1i – 1l) shows strong statistically significant decreasing trends in the Congo Basin, consistent for all precipitation totals and frequency parameters. This single region is responsible for disproportionately large reductions in precipitation over tropical land areas, as no other land area exhibits such a consistent negative change in precipitation across multiple components.

Decreasing precipitation trends in the Congo Basin have been reported in many studies in the last two decades (Hua et al., 2016; Jiang et al., 2019; Obarein & Lee, 2022). Other proxies, such as rainforest greenness (Zhou et al., 2014) and cloud cover (Lee, 2020), have also shown decreasing trends. Tropical forests play a vital role in modulating local, regional, and global climate through their impact on energy, water, and carbon cycles (Bonan, 2008; Staal et al., 2018). The Congo Basin has one of the highest precipitation recycling rates globally, with Baker and Spracklen (2022) estimating that about 50% of mean precipitation comes from evapotranspiration in the basin. Deforestation reduces evapotranspiration, which decreases precipitation (Lawrence & Vandecar, 2015; Leite-Filho et al., 2021; Nogherotto et al., 2013). Since trees generally have a lower albedo than cleared lands, deforestation alters the surface energy

balance via changes in latent heat/sensible heat flux. Moreover, removing forests by burning destroys essential carbon sinks and releases the stored carbon into the atmosphere enabling more warming.

Smith et al. (2023) assessed precipitation responses to deforestation at different spatial scales and found a 0.21 ± 0.19 mm decrease in precipitation per month for each 1% loss of forest cover. With future deforestation, they estimate that this drying trend could rise to 16.5 ± 6.2 mm per month by the end of the 21st century.

Like the Arctic, in-situ observations are sparse and unreliable over the Congo Basin due to its remote location, political and social unrest, and economic constraints. But despite these challenges, the drying trend appears robust in gridded observations (Hua et al., 2016) and in other reanalysis datasets (Jiang et al., 2019).

4 Conclusions

In this study, we analyzed multiple parameters of global precipitation change, showing that the ERA5 reanalysis dataset can reproduce some of the well-known signals of change at global and regional scales. Because precipitation is arguably the most conspicuous climate element, the largest impact of future climate changes on societies and ecosystems will likely come from precipitation variability and change. For instance, strong positive changes in precipitation extremes trigger flash floods, soil erosion, and landslides, especially in mountainous regions. It can also destroy plant and animal ecosystems, damage human infrastructure, and contaminate drinking water sources.

The intensification of precipitation extremes with little to no corresponding increase in total precipitation translates into strong decreases in wet days in most land areas. Decreasing wet days may lead to drought conditions that may reduce river water levels, deplete reservoirs and groundwater, and drive scarcity in drinking water supply. Accessibility to clean water is linked to sanitation and health, a significant challenge in the poorest places on Earth, and that may worsen if current dry trends persist. Recent shifts from snowfall to a rainfall regime in the mid-to-high-

latitudes mean less snow accumulation, requiring less energy to thaw, earlier snowmelt, and more immediate runoff, potentially leading to flooding.

Global precipitation studies are generally less common than local ones because the latter can be tailored to local concerns where impact is greatest, with finer resolution datasets that may show unique characteristics in precipitation patterns averaged out in global analyses. Yet global studies provide a broad overview of precipitation patterns, identify large-scale drivers, and highlight the interconnectedness of Earth's climate. More importantly, global studies allow comparison among different regions through the use of common methodologies and consistent data sources, thereby ensuring uniformity of findings. Possible future directions involve examining how teleconnective oscillations (e.g., ENSO, AMO, PDO) might play a role in the variability of the precipitation components examined here.

An important limitation in the use of ERA5 reanalysis datasets is that trends may be susceptible to time-dependent biases in the reanalysis, particularly those related to the types and quality of assimilated observations, and to model changes.

Acknowledgements

The authors would like to thank all the data providers for their efforts in making their datasets publicly available.

Data availability statement

The ERA5 data set is available at:
https://cds.climate.copernicus.eu/cdsapp#!/dataset/reanalysis-era5-single-levels?tab=form

Code availability

MATLAB and R language was used for coding the methods as described in the Data and Methods section and these are available on the first author's Github account https://github.com/Omon-Obarein/ERA5-REPRODUCES-KEY-FEATURES-OF-GLOBAL-PRECIPITATION-CHANGE-IN-A-WARMING-CLIMATE.git

Conflict of interest

The authors declare no conflict of interest

Funding Statement

No funding was used for this research

References

Adler, R. F., Gu, G., Sapiano, M., Wang, J.-J., & Huffman, G. J. (2017). Global Precipitation: Means, Variations and Trends During the Satellite Era (1979–2014). *Surveys in Geophysics*, *38*(4), 679–699. https://doi.org/10.1007/s10712-017-9416-4

Ali, R., Kuriqi, A., Abubaker, S., & Kisi, O. (2019). Long-Term Trends and Seasonality Detection of the Observed Flow in Yangtze River Using Mann-Kendall and Sen's Innovative Trend Method. *Water*, *11*(9), Article 9. https://doi.org/10.3390/w11091855

Allan, R. P., Liu, C., Zahn, M., Lavers, D. A., Koukouvagias, E., & Bodas-Salcedo, A. (2014). Physically Consistent Responses of the Global Atmospheric Hydrological Cycle in Models and Observations. *Surveys in Geophysics*, *35*(3), 533–552. https://doi.org/10.1007/s10712-012-9213-z

Allen, M. R., & Ingram, W. J. (2002). Constraints on future changes in climate and the hydrologic cycle. *Nature*, *419*(6903), Article 6903. https://doi.org/10.1038/nature01092

Baker, J. C. A., & Spracklen, D. V. (2022). Divergent Representation of Precipitation Recycling in the Amazon and the Congo in CMIP6 Models. *Geophysical Research Letters*, *49*(10), e2021GL095136. https://doi.org/10.1029/2021GL095136

Banerjee, A., Chen, R., Meadows, M. E., Sengupta, D., Pathak, S., Xia, Z., & Mal, S. (2021). Tracking 21st century climate dynamics of the Third Pole: An analysis of topo-climate impacts on snow cover in the central Himalaya using Google Earth Engine. *International Journal of Applied Earth Observation and Geoinformation*, *103*, 102490. https://doi.org/10.1016/j.jag.2021.102490

Bao, J., Sherwood, S. C., Alexander, L. V., & Evans, J. P. (2017). Future increases in extreme precipitation exceed observed scaling rates. *Nature Climate Change*, *7*(2), Article 2. https://doi.org/10.1038/nclimate3201

Berg, A., Findell, K., Lintner, B., Giannini, A., Seneviratne, S. I., van den Hurk, B., Lorenz, R., Pitman, A., Hagemann, S., Meier, A., Cheruy, F., Ducharne, A., Malyshev, S., & Milly, P. C. D. (2016). Land–atmosphere feedbacks amplify aridity increase over land under global warming. *Nature Climate Change*, *6*(9), Article 9. https://doi.org/10.1038/nclimate3029

Bintanja, R. (2018). The impact of Arctic warming on increased rainfall. *Scientific Reports*, *8*(1), Article 1. https://doi.org/10.1038/s41598-018-34450-3

Bintanja, R., & Selten, F. M. (2014). Future increases in Arctic precipitation linked to local evaporation and sea-ice retreat. *Nature*, *509*(7501), Article 7501. https://doi.org/10.1038/nature13259

Blöschl, G., Hall, J., Viglione, A., Perdigão, R. A. P., Parajka, J., Merz, B., Lun, D., Arheimer, B., Aronica, G. T., Bilibashi, A., Boháč, M., Bonacci, O., Borga, M., Čanjevac, I., Castellarin, A., Chirico, G. B., Claps, P., Frolova, N., Ganora, D., … Živković, N. (2019). Changing climate both increases and decreases European river floods. *Nature*, *573*(7772), Article 7772. https://doi.org/10.1038/s41586-019-1495-6

Boisvert, L. N., Webster, M. A., Parker, C. L., & Forbes, R. M. (2023). Rainy Days in the Arctic. *Journal of Climate*, *36*(19), 6855–6878. https://doi.org/10.1175/JCLI-D-22-0428.1

Bonan, G. B. (2008). Forests and Climate Change: Forcings, Feedbacks, and the Climate Benefits of Forests. *Science*, *320*(5882), 1444–1449. https://doi.org/10.1126/science.1155121

Box, J. E., Colgan, W. T., Christensen, T. R., Schmidt, N. M., Lund, M., Parmentier, F.-J. W., Brown, R., Bhatt, U. S., Euskirchen, E. S., Romanovsky, V. E., Walsh, J. E., Overland, J. E., Wang, M., Corell, R. W., Meier, W. N., Wouters, B., Mernild, S., Mård, J., Pawlak, J., & Olsen, M. S. (2019). Key indicators of Arctic climate change: 1971–2017. *Environmental Research Letters*, *14*(4), 045010. https://doi.org/10.1088/1748-9326/aafc1b

Burt, J. E., Barber, G. M., & Rigby, D. L. (2009). *Elementary Statistics for Geographers*. Guilford Press.

Byrne, M. P., & O'Gorman, P. A. (2015). The Response of Precipitation Minus Evapotranspiration to Climate Warming: Why the "Wet-Get-Wetter, Dry-Get-Drier" Scaling Does Not Hold over Land. *Journal of Climate*, *28*(20), 8078–8092. https://doi.org/10.1175/JCLI-D-15-0369.1

Cai, Z., You, Q., Wu, F., Chen, H. W., Chen, D., & Cohen, J. (2021). Arctic Warming Revealed by Multiple CMIP6 Models: Evaluation of Historical Simulations and Quantification of Future Projection Uncertainties. *Journal of Climate*, *34*(12), 4871–4892. https://doi.org/10.1175/JCLI-D-20-0791.1

Centella-Artola, A., Bezanilla-Morlot, A., Taylor, M. A., Herrera, D. A., Martinez-Castro, D., Gouirand, I., Sierra-Lorenzo, M., Vichot-Llano, A., Stephenson, T., Fonseca, C., Campbell, J., & Alpizar, M. (2020). Evaluation of Sixteen Gridded Precipitation Datasets over the Caribbean Region Using Gauge Observations. *Atmosphere*, *11*(12), Article 12. https://doi.org/10.3390/atmos11121334

Chaudhary, S., Dhanya, C. T., & Vinnarasi, R. (2017). Dry and wet spell variability during monsoon in gauge-based gridded daily precipitation datasets over India. *Journal of Hydrology*, *546*, 204–218. https://doi.org/10.1016/j.jhydrol.2017.01.023

Chervenkov, H., & Slavov, K. (2019). Theil–Sen estimator vs. Ordinary least squares—Trend analysis for selected ETCCDI climate indices. *Comptes Rendus de l'Académie Bulgare Des Sciences: Sciences Mathématiques et Naturelles*, *72*, 47–54. https://doi.org/10.7546/CRABS.2019.01.06

Chinita, M. J., Richardson, M., Teixeira, J., & Miranda, P. M. A. (2021). Global mean frequency increases of daily and sub-daily heavy precipitation in ERA5. *Environmental Research Letters*, *16*(7), 074035. https://doi.org/10.1088/1748-9326/ac0caa

Chou, C., Neelin, J. D., Chen, C.-A., & Tu, J.-Y. (2009). Evaluating the "Rich-Get-Richer" Mechanism in Tropical Precipitation Change under Global Warming. *Journal of Climate*, *22*(8), 1982–2005. https://doi.org/10.1175/2008JCLI2471.1

Contractor, S., Donat, M. G., & Alexander, L. V. (2021). Changes in Observed Daily Precipitation over Global Land Areas since 1950. *Journal of Climate*, *34*(1), 3–19. https://doi.org/10.1175/JCLI-D-19-0965.1

Dai, A. (2006). Precipitation Characteristics in Eighteen Coupled Climate Models. *Journal of Climate*, *19*(18), 4605–4630. https://doi.org/10.1175/JCLI3884.1

Dang, X., Peng, H., Wang, X., & Zhang, H. (n.d.). *Theil-Sen Estimators in a Multiple Linear Regression Model*.

Donat, M. G., Lowry, A. L., Alexander, L. V., O'Gorman, P. A., & Maher, N. (2016). More extreme precipitation in the world's dry and wet regions. *Nature Climate Change*, *6*(5), Article 5. https://doi.org/10.1038/nclimate2941

El-Shaarawi, A. H., & Piegorsch, W. W. (2002). *Encyclopedia of Environmetrics*. John Wiley & Sons.

Emori, S., & Brown, S. J. (2005). Dynamic and thermodynamic changes in mean and extreme precipitation under changed climate. *Geophysical Research Letters*, *32*(17). https://doi.org/10.1029/2005GL023272

Fasullo, J. T. (2010). Robust Land–Ocean Contrasts in Energy and Water Cycle Feedbacks. *Journal of Climate*, *23*(17), 4677–4693. https://doi.org/10.1175/2010JCLI3451.1

Feng, H., & Zhang, M. (2015). Global land moisture trends: Drier in dry and wetter in wet over land. *Scientific Reports*, *5*(1), Article 1. https://doi.org/10.1038/srep18018

Feng, S., & Hu, Q. (2007). Changes in winter snowfall/precipitation ratio in the contiguous United States. *Journal of Geophysical Research: Atmospheres*, *112*(D15). https://doi.org/10.1029/2007JD008397

Fischer, E. M., Sedláček, J., Hawkins, E., & Knutti, R. (2014). Models agree on forced response pattern of precipitation and temperature extremes. *Geophysical Research Letters*, *41*(23), 8554–8562. https://doi.org/10.1002/2014GL062018

Francis, J. A., & Vavrus, S. J. (2015). Evidence for a wavier jet stream in response to rapid Arctic warming. *Environmental Research Letters*, *10*(1), 014005. https://doi.org/10.1088/1748-9326/10/1/014005

Gleixner, S., Demissie, T., & Diro, G. T. (2020). Did ERA5 Improve Temperature and Precipitation Reanalysis over East Africa? *Atmosphere*, *11*(9), Article 9. https://doi.org/10.3390/atmos11090996

Greve, P., Orlowsky, B., Mueller, B., Sheffield, J., Reichstein, M., & Seneviratne, S. I. (2014). Global assessment of trends in wetting and drying over land. *Nature Geoscience*, *7*(10), Article 10. https://doi.org/10.1038/ngeo2247

Gu, L., Yin, J., Gentine, P., Wang, H.-M., Slater, L. J., Sullivan, S. C., Chen, J., Zscheischler, J., & Guo, S. (2023). Large anomalies in future extreme precipitation sensitivity driven by atmospheric dynamics. *Nature Communications*, *14*(1), Article 1. https://doi.org/10.1038/s41467-023-39039-7

Hamed, K. H., & Ramachandra Rao, A. (1998). A modified Mann-Kendall trend test for autocorrelated data. *Journal of Hydrology*, *204*(1), 182–196. https://doi.org/10.1016/S0022-1694(97)00125-X

Han, W., Xiao, C., Dou, T., & Ding, M. (2018). Changes in the Proportion of Precipitation Occurring as Rain in Northern Canada during Spring–Summer from 1979–2015. *Advances in Atmospheric Sciences*, *35*(9), 1129–1136. https://doi.org/10.1007/s00376-018-7226-3

Held, I. M., & Soden, B. J. (2006). Robust Responses of the Hydrological Cycle to Global Warming. *Journal of Climate*, *19*(21), 5686–5699. https://doi.org/10.1175/JCLI3990.1

Hersbach, H., Bell, B., Berrisford, P., Hirahara, S., Horányi, A., Muñoz-Sabater, J., Nicolas, J., Peubey, C., Radu, R., Schepers, D., Simmons, A., Soci, C., Abdalla, S., Abellan, X., Balsamo, G., Bechtold, P., Biavati, G., Bidlot, J., Bonavita, M., … Thépaut, J.-N. (2020). The ERA5 global reanalysis. *Quarterly Journal of the Royal Meteorological Society*, *146*(730), 1999–2049. https://doi.org/10.1002/qj.3803

Hoffmann, L., Günther, G., Li, D., Stein, O., Wu, X., Griessbach, S., Heng, Y., Konopka, P., Müller, R., Vogel, B., & Wright, J. S. (2019). From ERA-Interim to ERA5: The considerable impact of ECMWF's next-generation reanalysis on Lagrangian transport simulations. *Atmospheric Chemistry and Physics*, *19*(5), 3097–3124. https://doi.org/10.5194/acp-19-3097-2019

Hua, W., Zhou, L., Chen, H., Nicholson, S. E., Raghavendra, A., & Jiang, Y. (2016). Possible causes of the Central Equatorial African long-term drought. *Environmental Research Letters*, *11*(12), 124002. https://doi.org/10.1088/1748-9326/11/12/124002

Huang, J., Chen, X., Xue, Y., Lin, J., & Zhang, J. (2017). Changing characteristics of wet/dry spells during 1961–2008 in Sichuan province, southwest China. *Theoretical and Applied Climatology*, *127*(1–2), 129–141. https://doi.org/10.1007/s00704-015-1621-9

Huntington, T. G. (2006). Evidence for intensification of the global water cycle: Review and synthesis. *Journal of Hydrology*, *319*(1), 83–95. https://doi.org/10.1016/j.jhydrol.2005.07.003

Huntington, T. G., Hodgkins, G. A., Keim, B. D., & Dudley, R. W. (2004). Changes in the Proportion of Precipitation Occurring as Snow in New England (1949–2000). *Journal of Climate*, *17*(13), 2626–2636. https://doi.org/10.1175/1520-0442(2004)017<2626:CITPOP>2.0.CO;2

Hynčica, M., & Huth, R. (2019). Long-term changes in precipitation phase in Europe in cold half year. *Atmospheric Research*, *227*, 79–88. https://doi.org/10.1016/j.atmosres.2019.04.032

Intergovernmental Panel on Climate Change (IPCC). (2014). *Climate Change 2013 – The Physical Science Basis: Working Group I Contribution to the Fifth Assessment Report of the Intergovernmental Panel on Climate Change*. Cambridge University Press. https://doi.org/10.1017/CBO9781107415324

Jacobs, P., Lenssen, N., Schmidt, G., & Rohde, R. (2021). *The Arctic Is Now Warming Four Times As Fast As the Rest of the Globe*. *2021*, A13E-02.

Jiang, Y., Zhou, L., Tucker, C. J., Raghavendra, A., Hua, W., Liu, Y. Y., & Joiner, J. (2019). Widespread increase of boreal summer dry season length over the Congo rainforest. *Nature Climate Change*, *9*(8), Article 8. https://doi.org/10.1038/s41558-019-0512-y

Jiao, D., Xu, N., Yang, F., & Xu, K. (2021). Evaluation of spatial-temporal variation performance of ERA5 precipitation data in China. *Scientific Reports*, *11*(1), Article 1. https://doi.org/10.1038/s41598-021-97432-y

Jouberton, A., Shaw, T. E., Miles, E., McCarthy, M., Fugger, S., Ren, S., Dehecq, A., Yang, W., & Pellicciotti, F. (2022). Warming-induced monsoon precipitation phase change intensifies glacier mass loss in the southeastern Tibetan Plateau. *Proceedings of the National Academy of Sciences*, *119*(37), e2109796119. https://doi.org/10.1073/pnas.2109796119

Kendon, E. J., Roberts, N. M., Fowler, H. J., Roberts, M. J., Chan, S. C., & Senior, C. A. (2014). Heavier summer downpours with climate change revealed by weather forecast resolution model. *Nature Climate Change*, *4*(7), Article 7. https://doi.org/10.1038/nclimate2258

Kharin, V. V., Zwiers, F. W., Zhang, X., & Wehner, M. (2013). Changes in temperature and precipitation extremes in the CMIP5 ensemble. *Climatic Change*, *119*(2), 345–357. https://doi.org/10.1007/s10584-013-0705-8

Kidd, C., Levizzani, V., & Laviola, S. (2010). Section II: Rainfall measurement and estimation. In F. Y. Testik & M. Gebremichael (Eds.), *Geophysical Monograph Series* (Vol. 191, pp. 127–158). American Geophysical Union. https://doi.org/10.1029/2009GM000920

737 Knowles, N., Dettinger, M. D., & Cayan, D. R. (2006). Trends in Snowfall versus Rainfall in the
738 Western United States. *Journal of Climate*, *19*(18), 4545–4559.
739 https://doi.org/10.1175/JCLI3850.1

740 Kopec, B. G., Feng, X., Michel, F. A., & Posmentier, E. S. (2016). Influence of sea ice on Arctic
741 precipitation. *Proceedings of the National Academy of Sciences*, *113*(1), 46–51.
742 https://doi.org/10.1073/pnas.1504633113

743 Landrum, L., & Holland, M. M. (2020). Extremes become routine in an emerging new Arctic.
744 *Nature Climate Change*, *10*(12), Article 12. https://doi.org/10.1038/s41558-020-0892-z

745 Lawrence, D., & Vandecar, K. (2015). Effects of tropical deforestation on climate and agriculture.
746 *Nature Climate Change*, *5*(1), Article 1. https://doi.org/10.1038/nclimate2430

747 Lee, C. C. (2020). Trends and Variability in Airmass Frequencies: Indicators of a Changing Climate.
748 *Journal of Climate*, *33*(19), 8603–8617. https://doi.org/10.1175/JCLI-D-20-0094.1

749 Lehmann, J., Mempel, F., & Coumou, D. (2018). Increased Occurrence of Record-Wet and Record-
750 Dry Months Reflect Changes in Mean Rainfall. *Geophysical Research Letters*, *45*(24),
751 13,468-13,476. https://doi.org/10.1029/2018GL079439

752 Leite-Filho, A. T., Soares-Filho, B. S., Davis, J. L., Abrahão, G. M., & Börner, J. (2021). Deforestation
753 reduces rainfall and agricultural revenues in the Brazilian Amazon. *Nature*
754 *Communications*, *12*(1), Article 1. https://doi.org/10.1038/s41467-021-22840-7

755 Lim, W. H., & Roderick, M. L. (2009). *An Atlas on Global Water Cycle: Based on the IPCC AR4*
756 *Climate Models*. ANU Press. https://doi.org/10.26530/OAPEN_458809

757 Liu, B., Chen, C., Lian, Y., Chen, J., & Chen, X. (2015). Long-term change of wet and dry climatic
758 conditions in the southwest karst area of China. *Global and Planetary Change*, *127*, 1–11.
759 https://doi.org/10.1016/j.gloplacha.2015.01.009

760 Liu, B., Chen, J., Lu, W., Chen, X., & Lian, Y. (2016). Spatiotemporal characteristics of precipitation
761 changes in the Pearl River Basin, China. *Theoretical and Applied Climatology*, *123*(3), 537–
762 550. https://doi.org/10.1007/s00704-015-1375-4

763 Malayeri, A. K., Saghafian, B., & Raziei, T. (2021). Performance evaluation of ERA5 precipitation
764 estimates across Iran. *Arabian Journal of Geosciences*, *14*(23), 2676.
765 https://doi.org/10.1007/s12517-021-09079-8

766 Martinkova, M., & Kysely, J. (2020). Overview of Observed Clausius-Clapeyron Scaling of Extreme
767 Precipitation in Midlatitudes. *Atmosphere*, *11*(8), Article 8.
768 https://doi.org/10.3390/atmos11080786

769 Masson-Delmotte, V. P., Zhai, P., Pirani, S. L., Connors, C., Péan, S., Berger, N., Caud, Y., Chen, L.,
770 Goldfarb, M. I., & Scheel Monteiro, P. M. (2021). *IPCC, 2021: Summary for Policymakers.*

In: Climate Change 2021: The Physical Science Basis. Contribution of Working Group I to the Sixth Assessment Report of the Intergovernmental Panel on Climate Change [Report]. Cambridge University Press, Cambridge, United Kingdom and New York, NY, USA. https://researchspace.csir.co.za/dspace/handle/10204/12710

Matiu, M., Crespi, A., Bertoldi, G., Carmagnola, C. M., Marty, C., Morin, S., Schöner, W., Cat Berro, D., Chiogna, G., De Gregorio, L., Kotlarski, S., Majone, B., Resch, G., Terzago, S., Valt, M., Beozzo, W., Cianfarra, P., Gouttevin, I., Marcolini, G., … Weilguni, V. (2021). Observed snow depth trends in the European Alps: 1971 to 2019. *The Cryosphere*, *15*(3), 1343–1382. https://doi.org/10.5194/tc-15-1343-2021

McCrystall, M. R., Stroeve, J., Serreze, M., Forbes, B. C., & Screen, J. A. (2021). New climate models reveal faster and larger increases in Arctic precipitation than previously projected. *Nature Communications*, *12*(1), Article 1. https://doi.org/10.1038/s41467-021-27031-y

Neelin, J. D., Martinez-Villalobos, C., Stechmann, S. N., Ahmed, F., Chen, G., Norris, J. M., Kuo, Y.-H., & Lenderink, G. (2022). Precipitation Extremes and Water Vapor. *Current Climate Change Reports*, *8*(1), 17–33. https://doi.org/10.1007/s40641-021-00177-z

Nogherotto, R., Coppola, E., Giorgi, F., & Mariotti, L. (2013). Impact of Congo Basin deforestation on the African monsoon. *Atmospheric Science Letters*, *14*(1), 45–51. https://doi.org/10.1002/asl2.416

Nogueira, M. (2020). Inter-comparison of ERA-5, ERA-interim and GPCP rainfall over the last 40 years: Process-based analysis of systematic and random differences. *Journal of Hydrology*, *583*, 124632. https://doi.org/10.1016/j.jhydrol.2020.124632

Obarein, O. A., & Lee, C. C. (2022). Differential signal of change among multiple components of West African rainfall. *Theoretical and Applied Climatology*, *149*(1), 379–399. https://doi.org/10.1007/s00704-022-04052-1

O'Gorman, P. A., & Schneider, T. (2009). The physical basis for increases in precipitation extremes in simulations of 21st-century climate change. *Proceedings of the National Academy of Sciences*, *106*(35), 14773–14777. https://doi.org/10.1073/pnas.0907610106

Ohlson, J. A., & Kim, S. (2015). Linear valuation without OLS: The Theil-Sen estimation approach. *Review of Accounting Studies*, *20*(1), 395–435. https://doi.org/10.1007/s11142-014-9300-0

Oke, T. R. (2002). *Boundary Layer Climates*. Routledge.

Oki, T., & Kanae, S. (2006). Global Hydrological Cycles and World Water Resources. *Science*, *313*(5790), 1068–1072. https://doi.org/10.1126/science.1128845

Olauson, J. (2018). ERA5: The new champion of wind power modelling? *Renewable Energy*, *126*, 322–331. https://doi.org/10.1016/j.renene.2018.03.056

Pant, N. C., Ravindra, R., Srivastava, D., & Thompson, L. (2018). The Himalayan cryosphere: Past and present variability of the 'third pole.' *Geological Society, London, Special Publications*, *462*(1), 1–6. https://doi.org/10.1144/SP462.13

Parker, C. L., Mooney, P. A., Webster, M. A., & Boisvert, L. N. (2022). The influence of recent and future climate change on spring Arctic cyclones. *Nature Communications*, *13*(1), Article 1. https://doi.org/10.1038/s41467-022-34126-7

Pendergrass, A. G., & Hartmann, D. L. (2014). Changes in the Distribution of Rain Frequency and Intensity in Response to Global Warming. *Journal of Climate*, *27*(22), 8372–8383. https://doi.org/10.1175/JCLI-D-14-00183.1

Pendergrass, A. G., & Knutti, R. (2018). The Uneven Nature of Daily Precipitation and Its Change. *Geophysical Research Letters*, *45*(21), 11,980-11,988. https://doi.org/10.1029/2018GL080298

Pfahl, S., O'Gorman, P. A., & Fischer, E. M. (2017). Understanding the regional pattern of projected future changes in extreme precipitation. *Nature Climate Change*, *7*(6), Article 6. https://doi.org/10.1038/nclimate3287

Prein, A. F., Rasmussen, R. M., Ikeda, K., Liu, C., Clark, M. P., & Holland, G. J. (2017). The future intensification of hourly precipitation extremes. *Nature Climate Change*, *7*(1), Article 1. https://doi.org/10.1038/nclimate3168

Randriatsara, H. H.-R. H., Hu, Z., Xu, X., Ayugi, B., Sian, K. T. C. L. K., Mumo, R., & Ongoma, V. (2022). Evaluation of gridded precipitation datasets over Madagascar. *International Journal of Climatology*, *42*(13), 7028–7046. https://doi.org/10.1002/joc.7628

Rantanen, M., Karpechko, A. Y., Lipponen, A., Nordling, K., Hyvärinen, O., Ruosteenoja, K., Vihma, T., & Laaksonen, A. (2022). The Arctic has warmed nearly four times faster than the globe since 1979. *Communications Earth & Environment*, *3*(1), Article 1. https://doi.org/10.1038/s43247-022-00498-3

Ribes, A., Thao, S., Vautard, R., Dubuisson, B., Somot, S., Colin, J., Planton, S., & Soubeyroux, J.-M. (2019). Observed increase in extreme daily rainfall in the French Mediterranean. *Climate Dynamics*, *52*(1), 1095–1114. https://doi.org/10.1007/s00382-018-4179-2

Rixen, C., & Rolando, A. (Eds.). (2013). *The Impacts of Skiing and Related Winter Recreational Activities on Mountain Environments*. BENTHAM SCIENCE PUBLISHERS. https://doi.org/10.2174/9781608054886113010l

Roderick, M. L., Sun, F., Lim, W. H., & Farquhar, G. D. (2014). A general framework for understanding the response of the water cycle to global warming over land and ocean. *Hydrology and Earth System Sciences*, *18*(5), 1575–1589. https://doi.org/10.5194/hess-18-1575-2014

Salzmann, M. (2016). Global warming without global mean precipitation increase? *Science Advances*, *2*(6), e1501572. https://doi.org/10.1126/sciadv.1501572

Schroeer, K., & Kirchengast, G. (2018). Sensitivity of extreme precipitation to temperature: The variability of scaling factors from a regional to local perspective. *Climate Dynamics*, *50*(11), 3981–3994. https://doi.org/10.1007/s00382-017-3857-9

Screen, J. A., & Simmonds, I. (2012). Declining summer snowfall in the Arctic: Causes, impacts and feedbacks. *Climate Dynamics*, *38*(11), 2243–2256. https://doi.org/10.1007/s00382-011-1105-2

Şen, Z. (2017). Innovative trend significance test and applications. *Theoretical and Applied Climatology*, *127*(3), 939–947. https://doi.org/10.1007/s00704-015-1681-x

Serreze, M. C., & Barry, R. G. (2011). Processes and impacts of Arctic amplification: A research synthesis. *Global and Planetary Change*, *77*(1), 85–96. https://doi.org/10.1016/j.gloplacha.2011.03.004

Shi, S., & Liu, G. (2021). The latitudinal dependence in the trend of snow event to precipitation event ratio. *Scientific Reports*, *11*(1), Article 1. https://doi.org/10.1038/s41598-021-97451-9

Smith, C., Baker, J. C. A., & Spracklen, D. V. (2023). Tropical deforestation causes large reductions in observed precipitation. *Nature*, *615*(7951), Article 7951. https://doi.org/10.1038/s41586-022-05690-1

Staal, A., Tuinenburg, O. A., Bosmans, J. H. C., Holmgren, M., van Nes, E. H., Scheffer, M., Zemp, D. C., & Dekker, S. C. (2018). Forest-rainfall cascades buffer against drought across the Amazon. *Nature Climate Change*, *8*(6), Article 6. https://doi.org/10.1038/s41558-018-0177-y

Stephens, G. L., & Hu, Y. (2010). Are climate-related changes to the character of global-mean precipitation predictable? *Environmental Research Letters*, *5*(2), 025209. https://doi.org/10.1088/1748-9326/5/2/025209

Sun, F., Roderick, M. L., & Farquhar, G. D. (2012). Changes in the variability of global land precipitation. *Geophysical Research Letters*, *39*(19). https://doi.org/10.1029/2012GL053369

Tan, X., Wu, X., Huang, Z., Fu, J., Tan, X., Deng, S., Liu, Y., Gan, T. Y., & Liu, B. (2023). Increasing global precipitation whiplash due to anthropogenic greenhouse gas emissions. *Nature Communications*, *14*(1), Article 1. https://doi.org/10.1038/s41467-023-38510-9

Thackeray, C. W., Hall, A., Norris, J., & Chen, D. (2022). Constraining the increased frequency of global precipitation extremes under warming. *Nature Climate Change*, *12*(5), Article 5. https://doi.org/10.1038/s41558-022-01329-1

876 Trenberth, K. (2011). Changes in precipitation with climate change. *Climate Research*, *47*(1), 123–
877 138. https://doi.org/10.3354/cr00953

878 Trenberth, K. E. (2014). Water Cycles and Climate Change. In B. Freedman (Ed.), *Global*
879 *Environmental Change* (pp. 31–37). Springer Netherlands. https://doi.org/10.1007/978-
880 94-007-5784-4_30

881 Trenberth, K. E., Dai, A., Rasmussen, R. M., & Parsons, D. B. (2003). The Changing Character of
882 Precipitation. *Bulletin of the American Meteorological Society*, *84*(9), 1205–1218.
883 https://doi.org/10.1175/BAMS-84-9-1205

884 Turco, M., & Llasat, M. C. (2011). Trends in indices of daily precipitation extremes in Catalonia
885 (NE Spain), 1951–2003. *Natural Hazards and Earth System Sciences*, *11*(12), 3213–3226.
886 https://doi.org/10.5194/nhess-11-3213-2011

887 Urraca, R., Huld, T., Gracia-Amillo, A., Martinez-de-Pison, F. J., Kaspar, F., & Sanz-Garcia, A. (2018).
888 Evaluation of global horizontal irradiance estimates from ERA5 and COSMO-REA6
889 reanalyses using ground and satellite-based data. *Solar Energy*, *164*, 339–354.
890 https://doi.org/10.1016/j.solener.2018.02.059

891 Utsumi, N., Seto, S., Kanae, S., Maeda, E. E., & Oki, T. (2011). Does higher surface temperature
892 intensify extreme precipitation? *Geophysical Research Letters*, *38*(16).
893 https://doi.org/10.1029/2011GL048426

894 Vaittinada Ayar, P., & Mailhot, A. (2021). Evolution of Dry and Wet Spells Under Climate Change
895 Over North-Eastern North America. *Journal of Geophysical Research: Atmospheres*,
896 *126*(5). https://doi.org/10.1029/2020JD033740

897 Vergara-Temprado, J., Ban, N., & Schär, C. (2021). Extreme Sub-Hourly Precipitation Intensities
898 Scale Close to the Clausius-Clapeyron Rate Over Europe. *Geophysical Research Letters*,
899 *48*(3), e2020GL089506. https://doi.org/10.1029/2020GL089506

900 Visser, J. B., Wasko, C., Sharma, A., & Nathan, R. (2020). Resolving Inconsistencies in Extreme
901 Precipitation-Temperature Sensitivities. *Geophysical Research Letters*, *47*(18),
902 e2020GL089723. https://doi.org/10.1029/2020GL089723

903 Wang, B., Li, X., Huang, Y., & Zhai, G. (2016). Decadal trends of the annual amplitude of global
904 precipitation: Decadal trends of the annual amplitude of global precipitation.
905 *Atmospheric Science Letters*, *17*(1), 96–101. https://doi.org/10.1002/asl.631

906 Wang, Y., & Zhao, N. (2022). Evaluation of Eight High-Resolution Gridded Precipitation Products
907 in the Heihe River Basin, Northwest China. *Remote Sensing*, *14*(6), Article 6.
908 https://doi.org/10.3390/rs14061458

Webster, M. A., DuVivier, A. K., Holland, M. M., & Bailey, D. A. (2021). Snow on Arctic Sea Ice in a Warming Climate as Simulated in CESM. *Journal of Geophysical Research: Oceans*, *126*(1), e2020JC016308. https://doi.org/10.1029/2020JC016308

Westra, S., Alexander, L. V., & Zwiers, F. W. (2013). Global Increasing Trends in Annual Maximum Daily Precipitation. *Journal of Climate*, *26*(11), 3904–3918. https://doi.org/10.1175/JCLI-D-12-00502.1

Westra, S., Fowler, H. J., Evans, J. P., Alexander, L. V., Berg, P., Johnson, F., Kendon, E. J., Lenderink, G., & Roberts, N. M. (2014). Future changes to the intensity and frequency of short-duration extreme rainfall. *Reviews of Geophysics*, *52*(3), 522–555. https://doi.org/10.1002/2014RG000464

Wilks, D. S. (2016). "The Stippling Shows Statistically Significant Grid Points": How Research Results are Routinely Overstated and Overinterpreted, and What to Do about It. *Bulletin of the American Meteorological Society*, *97*(12), 2263–2273. https://doi.org/10.1175/BAMS-D-15-00267.1

Woods, C., & Caballero, R. (2016). The Role of Moist Intrusions in Winter Arctic Warming and Sea Ice Decline. *Journal of Climate*, *29*(12), 4473–4485. https://doi.org/10.1175/JCLI-D-15-0773.1

Wrzesien, M. L., Pavelsky, T. M., Sobolowski, S. P., Huning, L. S., Cohen, J. S., & Herman, J. D. (2022). Tracking the impacts of precipitation phase changes through the hydrologic cycle in snowy regions: From precipitation to reservoir storage. *Frontiers in Earth Science*, *10*. https://www.frontiersin.org/articles/10.3389/feart.2022.995874

Yu, L., & Zhong, S. (2021). Trends in Arctic seasonal and extreme precipitation in recent decades. *Theoretical and Applied Climatology*, *145*(3), 1541–1559. https://doi.org/10.1007/s00704-021-03717-7

Zhou, L., Tian, Y., Myneni, R. B., Ciais, P., Saatchi, S., Liu, Y. Y., Piao, S., Chen, H., Vermote, E. F., Song, C., & Hwang, T. (2014). Widespread decline of Congo rainforest greenness in the past decade. *Nature*, *509*(7498), Article 7498. https://doi.org/10.1038/nature13265

941 **SUPPLEMENTARY**

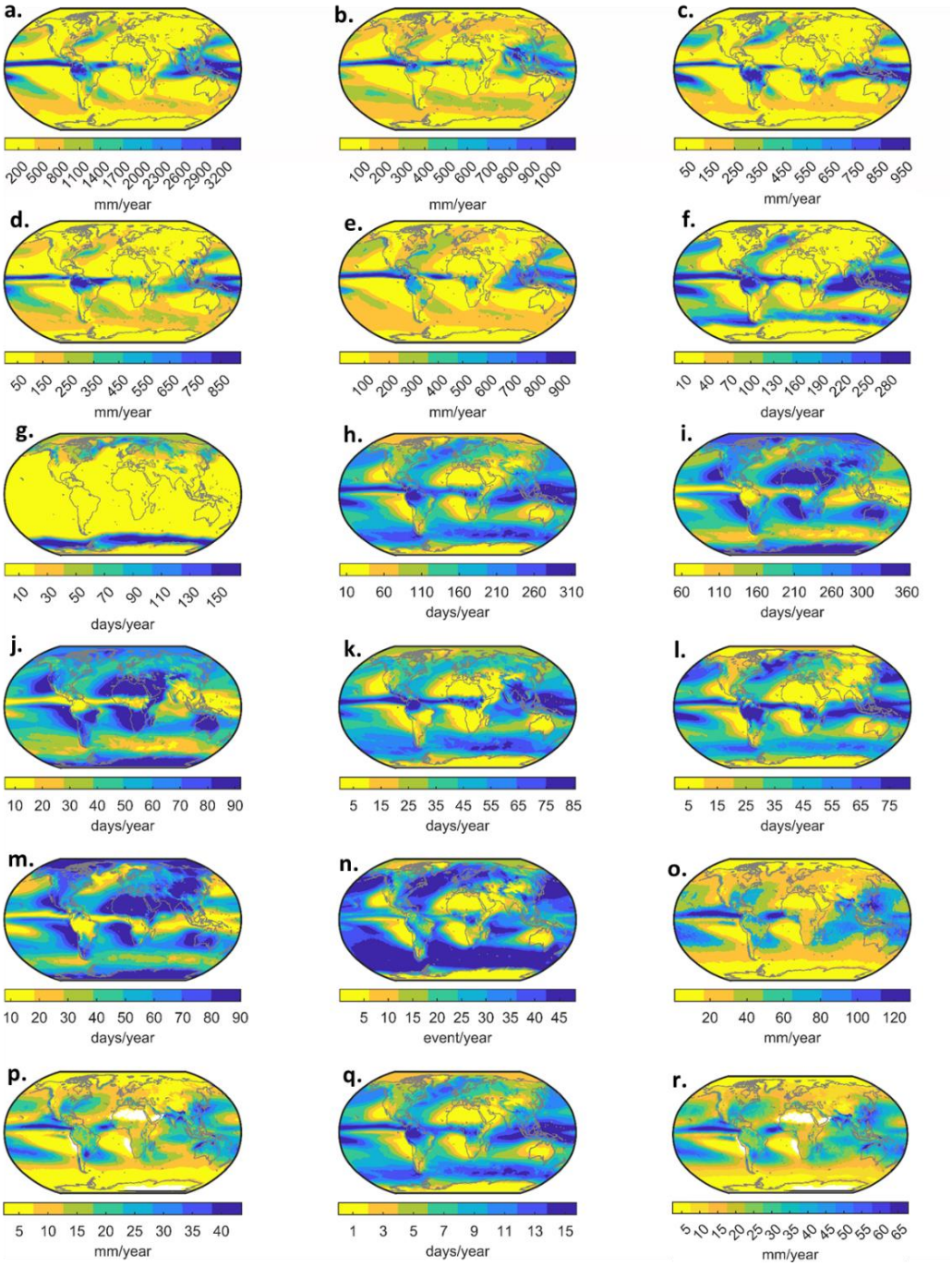

942

943 ***Figure A1****: Climatology of global (a) Annual precipitation totals; (b) Annual summer precipitation*
944 *totals; (c) Annual winter precipitation totals; (d) Annual spring precipitation totals; (e) Annual fall*
945 *precipitation totals; (f) Annual rain days; (g) Annual Snow days; (h) Annual wet days; (i) Annual*
946 *dry days; (j) Annual summer wet days; (k) Annual summer dry days; (l) Annual winter wet days;*
947 *(m) Annual winter dry days; (n) Annual wet spell; (o) Annual Maxima precipitation; (p) Annual*
948 *95th percentile precipitation; (q) Annual count of ≥ 95th percentile precipitation; and (r) Annual*
949 *median of ≥ 95th percentile precipitation, for the 1979 – 2022 period.*

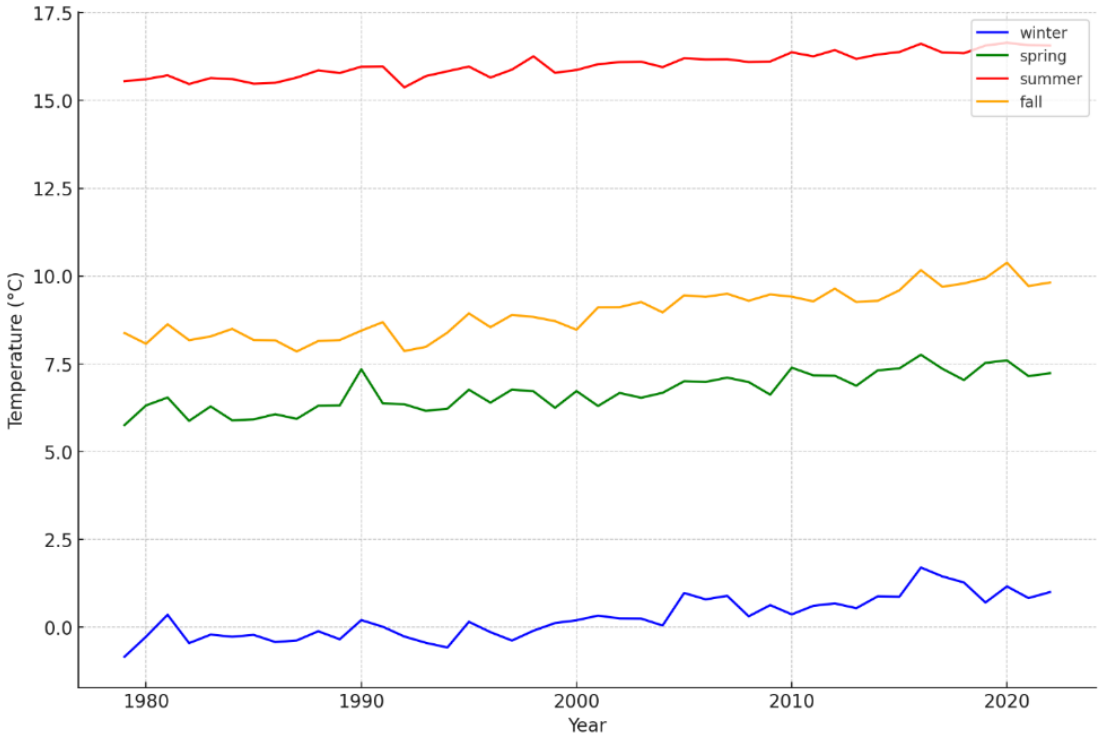

***Figure A2**: Seasonally-averaged mean monthly temperatures for the Northern Hemisphere (ERA5, 1979 - 2022).*

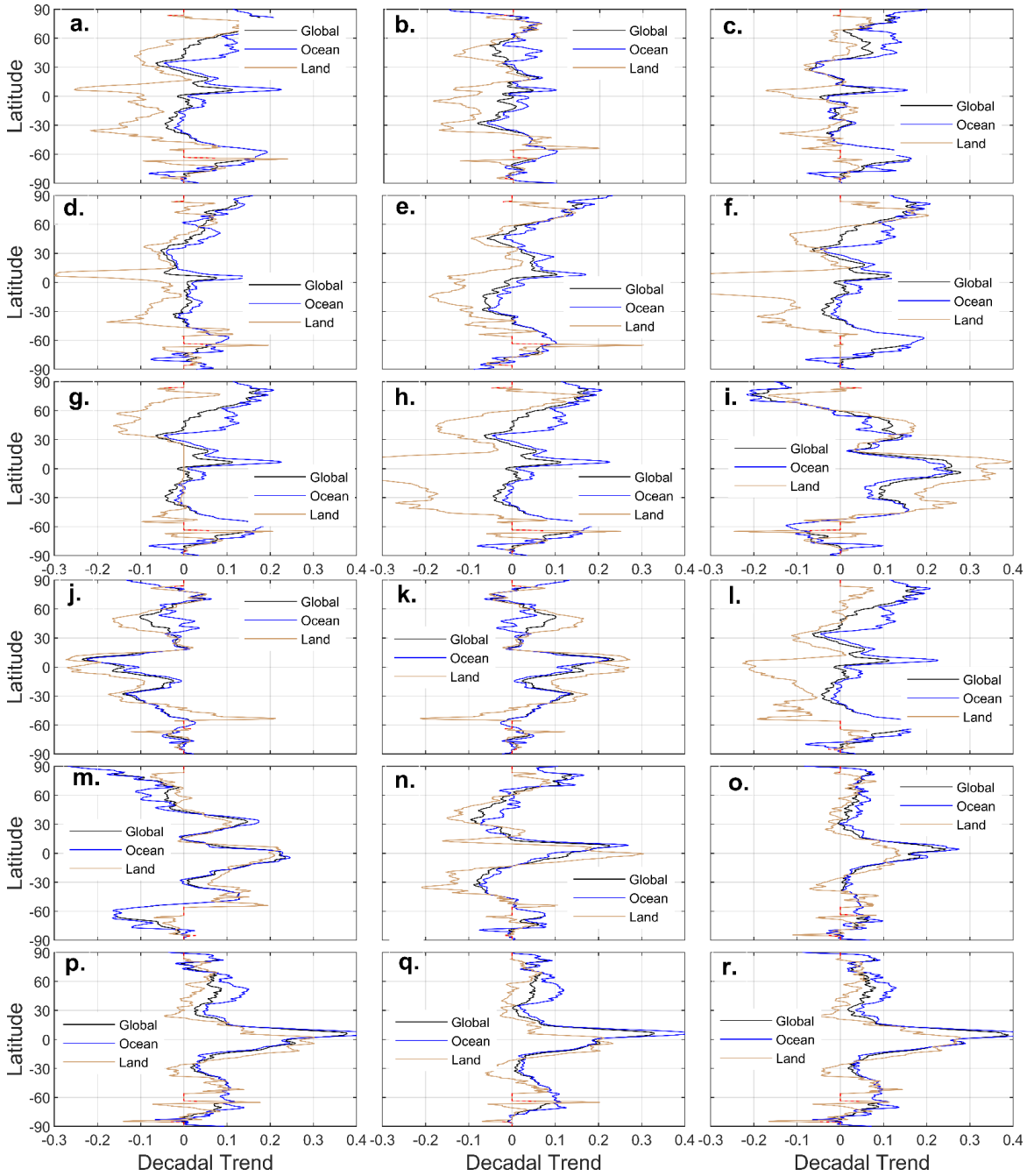

***Figure A3**: Global trends by latitude, global, ocean, land grid points (1979 - 2022) in (a) Annual precipitation totals; (b) Annual summer precipitation totals; (c) Annual winter precipitation totals; (d) Annual spring precipitation totals; (e) Annual fall precipitation totals; (f) Annual rain days; (g) Annual Snow days; (h) Annual wet days; (i) Annual dry days; (j) Annual summer wet days; (k) Annual summer dry days; (l) Annual winter wet days; (m) Annual winter dry days; (n) Annual wet spell; (o) Annual Maxima precipitation; (p) Annual 95th percentile precipitation; (q) Annual count of ≥ 95th percentile precipitation; and (r) Annual median of ≥ 95th percentile precipitation. Black stippling indicates statistically significant grid points. All trends are decadal and in standard deviation (z-scores) units.*

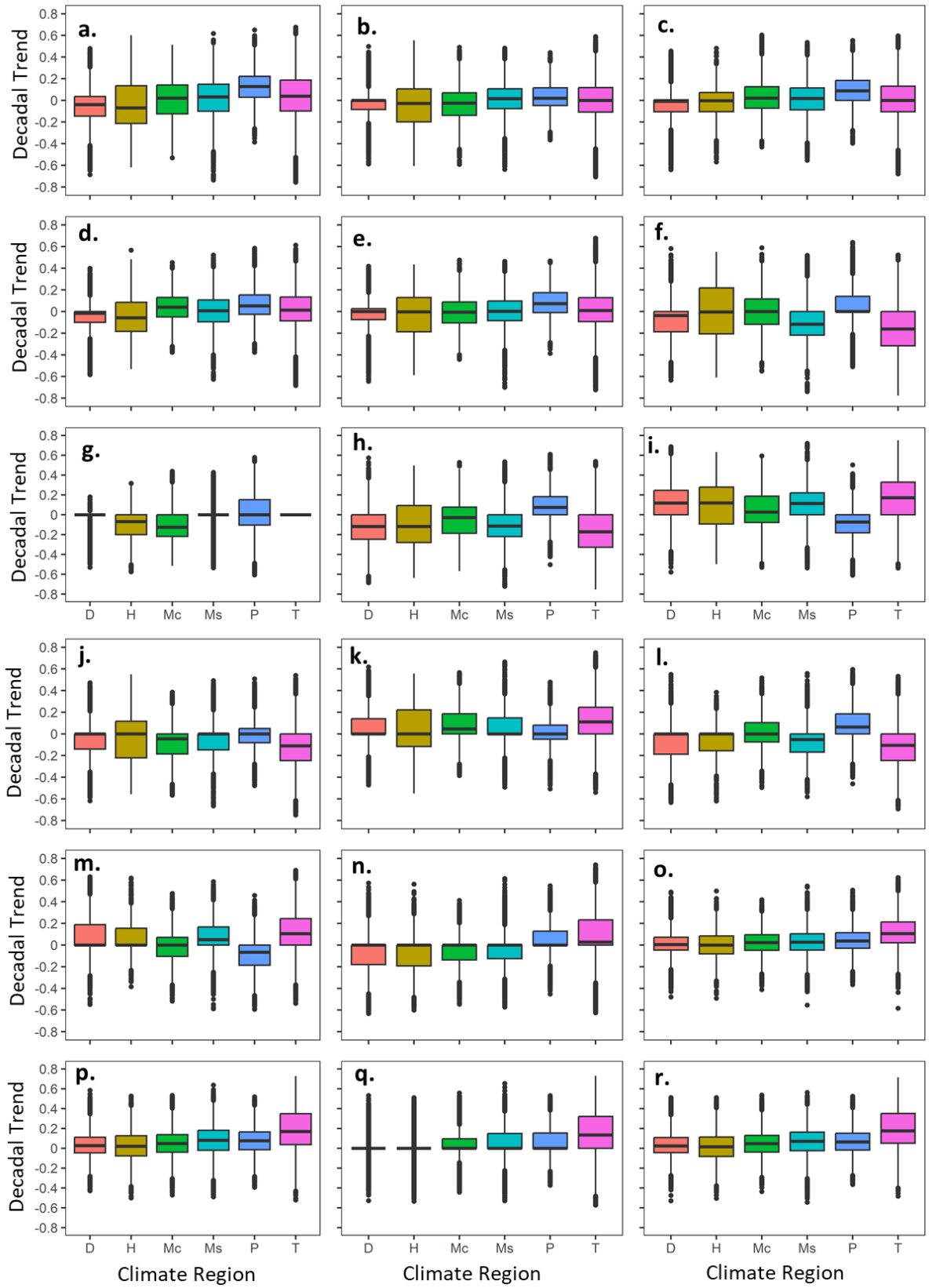
a.
b.
c.
d.
e.
f.
g.
h.
i.
j.
k.
l.
m.
n.
o.
p.
q.
r.
Decadal Trend
0.8
0.6
0.4
0.2
0
-0.2
-0.4
-0.6
-0.8
D
H
Mc
Ms
P
T
Climate Region

969

970 ***Figure A4****: Global trends by Climate region (1979 - 2022) in (a) Annual precipitation totals; (b)*
971 *Annual summer precipitation totals; (c) Annual winter precipitation totals; (d) Annual spring*
972 *precipitation totals; (e) Annual fall precipitation totals; (f) Annual rain days; (g) Annual Snow days;*
973 *(h) Annual wet days; (i) Annual dry days; (j) Annual summer wet days; (k) Annual summer dry*
974 *days; (l) Annual winter wet days; (m) Annual winter dry days; (n) Annual wet spell; (o) Annual*
975 *Maxima precipitation; (p) Annual 95th percentile precipitation; (q) Annual count of ≥ 95th*
976 *percentile precipitation; and (r) Annual median of ≥ 95th percentile precipitation. Black stippling*
977 *indicates statistically significant grid points. All trends are decadal and in standard deviation (z-*
978 *scores) units. Climate Region: T = Tropical; D = Dry Climate; Mc = Microthermal Climate;*
979 *Mesothermal Climate; P = Polar Climate; H = Highland Climate)*
980